Symmetric and non-symmetric discontinuous Galerkin methods for a pseudostress formulation of the Stokes spectral problem.

Felipe Lepe[a], David Mora[b,c]

[a] *Departamento de Matemática, Universidad Federico Santa María, Campus San Joaquín, Santiago, Chile.*

[b] *Departamento de Matemáticas, Universidad del Bío-Bío, Concepción, Chile.*

[c] *CI^{2}MA, Universidad de Concepción, Concepción, Chile.*

Abstract

In this paper we introduce and analyze symmetric and non-symmetric discontinuous Galerkin methods for the Stokes eigenvalue problem. The formulation is obtained by introducing the so-called pseudostress tensor and thanks to the structure of the system, the velocity and pressure variables are eliminated. We propose different DG discretizations to solve the resulting spectral problem and the convergence analysis is based on the abstract spectral theory for non-compact operators. We show that the proposed method is spurious modes free and asymptotic estimates for the eigenvalues and eigenfunctions are proved if the so-called stabilization parameter is sufficiently large and the meshsize is small enough. We report some numerical experiments to assess the performance of the methods.

Key words: Stokes eigenvalue problem, discontinuous Galerkin methods, error estimates.
AMS Subject Classification: 65N30, 65N12, 65N25, 76D07, 35Q35

1. Introduction

The discontinuous Galerkin method (DG) has taken relevance in the recent years to solve spectral problems (see for instance [1, 5, 6, 14, 16]). Compared with conforming finite elements, discretisations based on DG methods have a number of attractive features. For instance, the DG method has the advantage of being flexible in the choice of polynomial degrees, amenable for hp-adaptivity and relatively simple implementation on highly unstructured meshes. In particular, in [1], DG methods (symmetric and non-symmetric methods) have been introduced an analyzed for the Laplace eigenvalue problem. They have proved that for the Hermitian case is possible to obtain a double order of convergence for the eigenvalues but suboptimal order of convergence for the non-Hermitian cases. On the other hand, a complete analysis for Maxwell's eigenvalue problem has been presented in [6]. The authors have established necessary and sufficient conditions for a spurious free approximation by an H(curl) interior penalty discontinuous Galerkin method. More recently, a symmetric DG method has been presented and analyzed in [16] for the elasticity eigenproblem with reduced symmetry. It has been shown that the proposed scheme provides a correct approximation of the spectrum and prove asymptotic error estimates for the eigenvalues and the eigenfunctions. Additionaly in [14], an H(div)-conforming DG method has been studied for the classical velocity-pressure formulation of the Stokes eigenvalue problem. They proved a priori error estimates for

Email addresses: felipe.lepe@usm.cl (Felipe Lepe), dmora@ubiobio.cl (David Mora)

the eigenvalues and eigenfunctions. Moreover, an a posteriori error estimator of residual type is presented.

Now, following the recent work [16], we here propose a new DG discretization for the Stokes eigenvalue problem, which is based on so-called pseudostress tensor (non-symmetric) of the problem. We mention that the Stokes eigenvalue problem has attracted much interest since it is frequently encountered in important applications. For instance, to study the stability of fluid flow problems and it also appears in the study of the buckling problem of thin plates (see [22]). For that reason, different finite element formulations to solve this eigenvalue problem have been studied in the past years. Among the papers on this subject, we cite the following as a minimal sample [22, 2, 13, 15, 18, 21, 23].

The purpose of the present paper is to introduce and analyze a DG discretization for solving the Stokes eigenvalue problem. We consider a variational formulation of the problem written in H(div) as in [21], where an auxiliary variable is introduced, the non-symmetric pseudostress tensor, and the velocity and pressure are eliminated from the system. We introduce DG discretisations to approximate the pseudostress tensor by discontinuous finite element spaces of degree $k \geq 1$. Then, we use the abstract spectral theory for non-compact operators (see [8, 9]) to deal with the continuous and discrete solution operators, which appear as the solution of the continuous and discrete source problems, and whose spectra are related with the solutions of the eigenvalue problems. We prove stability of the DG discrete methods considering its symmetric and non-symmetric nature. This stability will depend on the choice of the so-called stabilization parameter. Then, we establish that the resulting DG discretizations provide a correct approximation of the spectrum if the stabilization parameter is sufficiently large and the meshsize h is small enough. We prove optimal order error estimates for the eigenfunctions and a double order for the eigenvalues in the symmetric case and sub-optimal order for the non-symmetric methods (cf Theorem 4.4). In particular, we will see in the numerical tests that the order of convergence for the non-symmetric methods depend on the choice of the polynomial degree: if the polynomial degree k is odd the convergence order is k and, if k is even, the convergence order is $k+1$. We will also see that the methods can be affected by the presence of spurious modes if the stabilization parameters are not chosen appropiately.

The outline of the paper is the following: in Section 2, we describe the continuous problem in terms of the pseudostress tensor. We recall the spectral characterization of the corresponding solution operator and the regularity results proved in [21]. In Section 3, we introduce the DG methods, describing the spaces, the discrete norms and the general framework. We also prove the stability of the DG methods and we introduce the discrete solution operator. Section 4 is dedicated to prove error estimates for the eigenfunctions and eigenvalues. In Section 5, we present some numerical test to assess the performance of the proposed DG methods. Finally, we summarize some conclusions in Section 6.

We end this section with some of the notations that we will use below. Given any Hilbert space V, let V^n and $V^{n\times n}$ denote, respectively, the space of vectors and tensors of order n ($n = 2, 3$) with entries in V. In particular, $\boldsymbol{I}$ is the identity matrix of $\mathbb{R}^{n\times n}$ and $\mathbf{0}$ denotes a generic null vector or tensor. Given $\boldsymbol{\tau} := (\tau_{ij})$ and $\boldsymbol{s} := (s_{ij}) \in \mathbb{R}^{n\times n}$, we define as usual the transpose tensor $\boldsymbol{\tau}^{\mathtt{t}} := (\tau_{ji})$, the trace $\operatorname{tr}\boldsymbol{\tau} := \sum_{i=1}^{n} \tau_{ii}$, the deviatoric tensor $\boldsymbol{\tau}^{\mathtt{D}} := \boldsymbol{\tau} - \frac{1}{n}(\operatorname{tr}\boldsymbol{\tau})\,\boldsymbol{I}$, and the tensor inner product $\boldsymbol{\tau} : \boldsymbol{s} := \sum_{i,j=1}^{n} \tau_{ij} s_{ij}$.

Let Ω be a polyhedral Lipschitz bounded domain of $\mathbb{R}^n$ with boundary $\partial\Omega$. For $s \geq 0$, $\|\cdot\|_{s,\Omega}$ stands indistinctly for the norm of the Hilbertian Sobolev spaces $\mathrm{H}^s(\Omega)$, $\mathrm{H}^s(\Omega)^n$ or $\mathrm{H}^s(\Omega)^{n\times n}$, with the convention $\mathrm{H}^0(\Omega) := \mathrm{L}^2(\Omega)$. We also define for $s \geq 0$ the Hilbert space $\mathrm{H}^s(\mathbf{div}, \Omega) := \{\boldsymbol{\tau} \in \mathrm{H}^s(\Omega)^{n\times n} : \ \mathbf{div}\,\boldsymbol{\tau} \in \mathrm{H}^s(\Omega)^n\}$, whose norm is given by $\|\boldsymbol{\tau}\|^2_{\mathrm{H}^s(\mathbf{div},\Omega)} := \|\boldsymbol{\tau}\|^2_{s,\Omega} + \|\mathbf{div}\,\boldsymbol{\tau}\|^2_{s,\Omega}$ and denote $\mathrm{H}(\mathbf{div}, \Omega) := \mathrm{H}^0(\mathbf{div}; \Omega)$.

2. The continuous spectral problem

Let $\Omega \subset \mathbb{R}^n$, with $n = 2, 3$, be a bounded and connected Lipschitz domain. We denote by $\boldsymbol{n}$ the outward unit normal vector to $\Gamma := \partial\Omega$ and assume that Γ admits a disjoint partition $\Gamma := \Gamma_D \cup \Gamma_N$, we also assume that both Γ_D and Γ_N have positive measure.

In what follows, we recall the variational formulation of the Stokes eigenvalue problem proposed in [21]. Also, we summarize some results from this reference.

The Stokes eigenvalue model problem of our interest is the following: Find nontrivial $(\widehat{\lambda}, \boldsymbol{u}, p)$ such that (see [18])

$$\begin{aligned} -\,\mathbf{div}(\nabla \boldsymbol{u}) + \nabla p &= \widehat{\lambda}\boldsymbol{u} && \text{in}\,\Omega, \\ \operatorname{div} \boldsymbol{u} &= 0 && \text{in}\,\Omega, \\ \boldsymbol{u} &= \boldsymbol{0} && \text{on}\,\Gamma_D, \\ (\nabla \boldsymbol{u} - p\boldsymbol{I})\boldsymbol{n} &= \boldsymbol{0} && \text{on}\,\Gamma_N. \end{aligned} \tag{2.1}$$

To study this problem, we introduce the so-called pseudostress tensor $\boldsymbol{\sigma} := \nabla \boldsymbol{u} - p\boldsymbol{I}$ (see [7, 11, 12]), which will be sought in the following functional space

$$\boldsymbol{\mathcal{V}} := \{\boldsymbol{\tau} \in \mathrm{H}(\mathbf{div}, \Omega) : \boldsymbol{\tau}\boldsymbol{n} = \boldsymbol{0} \ \text{ on } \ \Gamma_N\}.$$

Then, we eliminate the pressure p and the velocity $\boldsymbol{u}$ from the above system (see [21] for further details), to write the following eigenvalue problem: Find $\lambda \in \mathbb{R}$ and $\boldsymbol{0} \neq \boldsymbol{\sigma} \in \boldsymbol{\mathcal{V}}$ such that

$$a(\boldsymbol{\sigma}, \boldsymbol{\tau}) = \lambda b(\boldsymbol{\sigma}, \boldsymbol{\tau}) \qquad \forall \boldsymbol{\tau} \in \boldsymbol{\mathcal{V}}, \tag{2.2}$$

where $\lambda := 1 + \widehat{\lambda}$ and the bilinear forms $a : \boldsymbol{\mathcal{V}} \times \boldsymbol{\mathcal{V}} \to \mathbb{R}$ and $b : \boldsymbol{\mathcal{V}} \times \boldsymbol{\mathcal{V}} \to \mathbb{R}$ are defined as

$$\begin{aligned} a(\boldsymbol{\sigma}, \boldsymbol{\tau}) &:= \int_\Omega \mathbf{div}\, \boldsymbol{\sigma} \cdot \mathbf{div}\, \boldsymbol{\tau} + \int_\Omega \boldsymbol{\sigma}^{\mathtt{D}} : \boldsymbol{\tau}^{\mathtt{D}}, \\ b(\boldsymbol{\sigma}, \boldsymbol{\tau}) &:= \int_\Omega \boldsymbol{\sigma}^{\mathtt{D}} : \boldsymbol{\tau}^{\mathtt{D}}. \end{aligned}$$

We note that a shift argument has been used to write (2.2). This has been done in order to analyze the variational formulation with a well-posed solution operator (cf. (2.3)).

The bilinear form a is $\boldsymbol{\mathcal{V}}$-elliptic as stated in the following result.

Lemma 2.1. *There exists a constant $\alpha > 0$, depending only on Ω, such that*

$$a(\boldsymbol{\tau}, \boldsymbol{\tau}) \geq \alpha \|\boldsymbol{\tau}\|^2_{\mathbf{div},\Omega} \qquad \forall \boldsymbol{\tau} \in \boldsymbol{\mathcal{V}}.$$

Proof. See Lemma 2.1 in [20]. □

According to Lemma 2.1, we are in position to introduce the following solution operator $\boldsymbol{T}$, defined as follows:

$$\begin{aligned} \boldsymbol{T} : \boldsymbol{\mathcal{V}} &\to \boldsymbol{\mathcal{V}}, \\ \boldsymbol{f} &\mapsto \boldsymbol{T}\boldsymbol{f} := \widetilde{\boldsymbol{\sigma}}, \end{aligned} \tag{2.3}$$

where $\widetilde{\boldsymbol{\sigma}} \in \boldsymbol{\mathcal{V}}$ is the unique solution, as a consequence of Lemma 2.1 and the Lax-Milgram Theorem, of the following source problem:

$$a(\widetilde{\boldsymbol{\sigma}}, \boldsymbol{\tau}) = b(\boldsymbol{f}, \boldsymbol{\tau}) \qquad \forall \boldsymbol{\tau} \in \boldsymbol{\mathcal{V}}. \tag{2.4}$$

Thus, we have that the linear operator $\boldsymbol{T}$ is well defined and bounded. Clearly $(\lambda, \boldsymbol{\sigma}) \in \mathbb{R} \times \boldsymbol{\mathcal{V}}$ solves problem (2.2) if and only of $(\mu = 1/\lambda, \boldsymbol{\sigma})$ is an eigenpair of $\boldsymbol{T}$, with $\mu \neq 0$ and $\boldsymbol{\sigma} \neq \mathbf{0}$. Moreover, the linear operator $\boldsymbol{T}$ is self-adjoint with respect to the inner product $a(\cdot, \cdot)$ in $\boldsymbol{\mathcal{V}}$.

Let

$$\boldsymbol{\mathcal{X}} := \{\boldsymbol{\tau} \in \boldsymbol{\mathcal{V}} : \mathbf{div}\, \boldsymbol{\tau} = \mathbf{0} \text{ in } \Omega\}. \tag{2.5}$$

It is clear that $\boldsymbol{T}|_{\boldsymbol{\mathcal{X}}} : \boldsymbol{\mathcal{X}} \to \boldsymbol{\mathcal{X}}$ reduces to the identity, leading to the conclusion that $\mu = 1$ is an eigenvalue of $\boldsymbol{T}$ with associated eigenspace $\boldsymbol{\mathcal{X}}$.

In reference [21] has been shown that there exists an operator $\boldsymbol{P} : \boldsymbol{\mathcal{V}} \to \boldsymbol{\mathcal{V}}$, which satisfies the following properties:

- $\boldsymbol{P}$ is idempotent and its kernel is given by $\boldsymbol{\mathcal{X}}$;
- There exist $C > 0$ and $s \in (0, 1]$ depending only on the geometry of Ω such that $\boldsymbol{P}(\boldsymbol{\mathcal{V}}) \subset \mathrm{H}^s(\Omega)^{n \times n}$ and $\|\boldsymbol{P}(\boldsymbol{\tau})\|_{s,\Omega} \leq C \|\mathbf{div}\, \boldsymbol{\tau}\|_{0,\Omega}$,
- $\boldsymbol{P}(\boldsymbol{\mathcal{V}})$ is invariant for $\boldsymbol{T}$. Moreover, $\boldsymbol{P}(\boldsymbol{\mathcal{V}})$ is orthogonal to $\boldsymbol{\mathcal{X}}$ with respect to the inner product $a(\cdot, \cdot)$ of $\boldsymbol{\mathcal{V}}$.

As an immediate consequence of the properties listed above, we have that the space $\boldsymbol{\mathcal{V}}$ can be decomposed in the following direct sum $\boldsymbol{\mathcal{V}} = \boldsymbol{\mathcal{X}} \oplus \boldsymbol{P}(\boldsymbol{\mathcal{V}})$. Moreover, we have the following regularity result, which proof follow the arguments of those in [21, Proposition 3.4].

Proposition 2.1. *There exists $s \in (0, 1]$ such that,*

$$\boldsymbol{T}(\boldsymbol{P}(\boldsymbol{\mathcal{V}})) \subset \{\boldsymbol{\tau} \in \mathrm{H}^s(\Omega)^{n \times n} : \mathbf{div}\, \boldsymbol{\tau} \in \mathrm{H}^{1+s}(\Omega)^n\},$$

and there exists $C > 0$ such that, for all $\boldsymbol{f} \in \boldsymbol{P}(\boldsymbol{\mathcal{V}})$, if $\boldsymbol{\sigma}^* = \boldsymbol{T}\boldsymbol{f}$, then

$$\|\boldsymbol{\sigma}^*\|_{s,\Omega} + \|\mathbf{div}\, \boldsymbol{\sigma}^*\|_{1+s,\Omega} \leq C \|\boldsymbol{f}\|_{\mathbf{div},\Omega},$$

concluding that $\boldsymbol{T}|_{\boldsymbol{P}(\boldsymbol{\mathcal{V}})} : \boldsymbol{P}(\boldsymbol{\mathcal{V}}) \to \boldsymbol{P}(\boldsymbol{\mathcal{V}})$ is compact.

All the previous results leads to the following spectral characterization of operator $\boldsymbol{T}$ proved in Theorem 3.5 of [21].

Lemma 2.2. *The spectrum of $\boldsymbol{T}$ decomposes as follows:* $\mathrm{sp}(\boldsymbol{T}) = \{0, 1\} \cup \{\mu_k\}_{k \in \mathbb{N}}$, *where*

- $\mu = 1$ *is an infinite-multiplicity eigenvalue of $\boldsymbol{T}$ and its associated eigenspace is $\boldsymbol{\mathcal{X}}$.*
- $\mu = 0$ *is an eigenvalue of $\boldsymbol{T}$ and its associated eigenspace is*

$$\mathcal{Z} := \{\boldsymbol{\tau} \in \boldsymbol{\mathcal{V}} : \boldsymbol{\tau}^{\mathtt{D}} = \mathbf{0}\} = \{qI : q \in \mathrm{H}^1(\Omega) \text{ and } q = 0 \text{ on } \Sigma\},$$

- $\{\mu_k\}_{k \in \mathbb{N}} \subset (0, 1)$ *is a sequence of nondefective finite-multiplicity eigenvalues of $\boldsymbol{T}$ which converge to 0.*

Moreover, the following additional regularity result holds true for eigenfunctions $\boldsymbol{\sigma}$ associated to some eigenvalue $\mu \in (0, 1)$. The proof follow from a classical bootstrap trick.

Proposition 2.2. *Let $\boldsymbol{\sigma} \in \boldsymbol{\mathcal{V}}$ be an eigenfunction associated with an eigenvalue $\mu \in (0, 1)$. Then, there exists a positive constant $C > 0$, depending on the eigenvalue, such that*

$$\|\boldsymbol{\sigma}\|_{r,\Omega} + \|\mathbf{div}\, \boldsymbol{\sigma}\|_{1+r,\Omega} \leq C \|\boldsymbol{\sigma}\|_{\mathbf{div},\Omega},$$

with $r > 0$.

3. The DG discretization

In this section we will introduce symmetric and non-symmetric DG discretizations to solve the Stokes eigenvalue problem. We start with standard definitions, then we introduce the DG spaces, jumps, averages, and the bilinear forms.

Let $\mathcal{T}_h$ be a shape regular family of meshes which subdivide the domain $\bar{\Omega}$ into triangles/tetrahedra K. Let h_K denote the diameter of the element K and h the maximum of the diameters of all the elements of the mesh, i.e. $h := \max_{K\in\mathcal{T}_h}\{h_K\}$.

Let F be a closed set. We say that $F \subset \overline{\Omega}$ is an interior edge/face if F has a positive $(n-1)$-dimensional measure and if there are distinct elements K and K' such that $F = \bar{K} \cap \bar{K}'$. A closed subset $F \subset \overline{\Omega}$ is a boundary edge/face if there exists $K \in \mathcal{T}_h$ such that F is an edge/face of K and $F = \bar{K} \cap \partial\Omega$. Let $\mathcal{F}_h^0$ and $\mathcal{F}_h^\partial$ be the sets of interior edges/faces and boundary edges/face, respectively. We assume that the boundary mesh $\mathcal{F}_h^\partial$ is compatible with the partition $\partial\Omega = \Gamma_D \cup \Gamma_N$; namely,

$$\bigcup_{F\in\mathcal{F}_h^D} F = \Gamma_D \qquad \text{and} \qquad \bigcup_{F\in\mathcal{F}_h^N} F = \Gamma_N,$$

where $\mathcal{F}_h^D := \{F \in \mathcal{F}_h^\partial; \quad F \subset \Gamma_D\}$ and $\mathcal{F}_h^N := \{F \in \mathcal{F}_h^\partial; \quad F \subset \Gamma_N\}$. Also we denote $\mathcal{F}_h := \mathcal{F}_h^0 \cup \mathcal{F}_h^\partial$ and $\mathcal{F}_h^* := \mathcal{F}_h^0 \cup \mathcal{F}_h^N$. Also, for any element $K \in \mathcal{T}_h$, we introduce the set $\mathcal{F}(K) := \{F \in \mathcal{F}_h; \quad F \subset \partial K\}$ of edges/faces composing the boundary of K.

Let $\mathbb{P}_m(\mathcal{T}_h)$ be the space of piecewise polynomials respect to $\mathcal{T}_h$ of degree at most $m \geq 0$; namely,

$$\mathbb{P}_m(\mathcal{T}_h) := \left\{v \in \mathrm{L}^2(\Omega); v|_K \in \mathbb{P}_m(K), \forall K \in \mathcal{T}_h\right\}.$$

For any $k \geq 1$, we define the finite element spaces $\boldsymbol{\mathcal{V}}_h := \mathbb{P}_k(\mathcal{T}_h)^{n\times n}$ and $\boldsymbol{\mathcal{V}}_h^c := \boldsymbol{\mathcal{V}}_h \cap \boldsymbol{\mathcal{V}}$. We observe that the space $\boldsymbol{\mathcal{V}}_h^c$ is the Brezzi-Douglas-Marini (BDM) finite element space. Now, we recall some well-known properties of the space $\boldsymbol{\mathcal{V}}_h^c$ (see [4]).

Let $\Pi_h : \mathrm{H}^t(\Omega)^{n\times n} \to \boldsymbol{\mathcal{V}}_h^c$ be he tensorial version of the BDM-interpolation operator , which satisfies the following classical error estimate, see [3, Proposition 2.5.4],

$$\|\boldsymbol{\tau} - \Pi_h\boldsymbol{\tau}\|_{0,\Omega} \leq Ch^{\min\{t,k+1\}}\|\boldsymbol{\tau}\|_{t,\Omega} \qquad \forall\boldsymbol{\tau} \in \mathrm{H}^t(\Omega)^{n\times n}, \quad t > 1/2. \tag{3.6}$$

Also, for less regular tensorial fields we have the following estimate

$$\|\boldsymbol{\tau} - \Pi_h\boldsymbol{\tau}\|_{0,\Omega} \leq Ch^t(\|\boldsymbol{\tau}\|_{t,\Omega} + \|\boldsymbol{\tau}\|_{\mathbf{div},\Omega}) \quad \forall\boldsymbol{\tau} \in \mathrm{H}^t(\Omega)^{n\times n} \cap \mathrm{H}(\mathbf{div},\Omega) \quad t \in (0, 1/2]. \tag{3.7}$$

Moreover, the following commuting diagram property holds true:

$$\|\mathbf{div}(\boldsymbol{\tau} - \Pi_h\boldsymbol{\tau})\|_{0,\Omega} = \|\mathbf{div}\,\boldsymbol{\tau} - \mathcal{R}_h\,\mathbf{div}\,\boldsymbol{\tau}\|_{0,\Omega} \leq Ch^{\min\{t,k\}}\|\mathbf{div}\,\boldsymbol{\tau}\|_{t,\Omega}, \tag{3.8}$$

for $\mathbf{div}\,\boldsymbol{\tau} \in \mathrm{H}^t(\Omega)^n$ and $\mathcal{R}_h$ being the $\mathrm{L}^2(\Omega)^n$-orthogonal projection onto $\mathbb{P}_{k-1}(\mathcal{T}_h)^n$.

For any $t \geq 0$, we define the following broken Sobolev space

$$\mathrm{H}^t(\mathcal{T}_h)^n := \{\boldsymbol{v} \in \mathrm{L}^2(\Omega)^n; \quad \boldsymbol{v}|_K \in \mathrm{H}^t(K)^n \quad \forall K \in \mathcal{T}_h\}.$$

Now, for $\boldsymbol{v} := \{\boldsymbol{v}_K\} \in \mathrm{H}^t(\mathcal{T}_h)^n$ and $\boldsymbol{\tau} := \{\boldsymbol{\tau}_K\} \in \mathrm{H}^t(\mathcal{T}_h)^{n\times n}$ the components $\boldsymbol{v}_K$ and $\boldsymbol{\tau}_K$ represent the restrictions $\boldsymbol{v}|_K$ and $\boldsymbol{\tau}|_K$ and, when it is convenient, we will drop the subscript for these restrictions. The space of the skeletons of the triangulations $\mathcal{T}_h$ is defined by $\mathrm{L}^2(\mathcal{F}_h) := \prod_{F\in\mathcal{F}_h}\mathrm{L}^2(F)$.

In the forthcoming analysis, $h_{\mathcal{F}} \in \mathrm{L}^2(\mathcal{F}_h)$ will represent the piecewise constant function defined by $h_{\mathcal{F}}|_F := h_F$ for all $F \in \mathcal{F}_h$, where h_F denotes the diameter of edge/face F.

Next, for $\boldsymbol{v} \in \mathrm{H}^t(\mathcal{T}_h)^n$, with $t > 1/2$, we define averages $\{\boldsymbol{v}\} \in \mathrm{L}^2(\mathcal{F}_h)^n$ and jumps $[\![\boldsymbol{v}]\!] \in \mathrm{L}^2(\mathcal{F}_h)$ as follows

$$\{\boldsymbol{v}\}_F := (\boldsymbol{v}_K + \boldsymbol{v}_{K'})/2 \quad \text{and} \quad [\![\boldsymbol{v}]\!]_F := \boldsymbol{v}_K \cdot \boldsymbol{n}_K + \boldsymbol{v}_{K'} \cdot \boldsymbol{n}_{K'} \quad \forall F \in \mathcal{F}(K) \cap \mathcal{F}(K'),$$

where $\boldsymbol{n}_K$ is the outward unit normal vector to ∂K. Also, on the boundary $\partial\Omega$ and for all $F \in \mathcal{F}(K) \cap \partial\Omega$, the averages and jumps are defined by $\{\boldsymbol{v}\}_F := \boldsymbol{v}_K$ and $[\![\boldsymbol{v}]\!]_F := \boldsymbol{v}_K \cdot \boldsymbol{n}$, respectively. For tensorial fields the previous definitions are analogous.

For a tensor field $\boldsymbol{\tau} \in \boldsymbol{\mathcal{V}}_h$ we define $\mathbf{div}_h\, \boldsymbol{\tau} \in \mathrm{L}^2(\Omega)^n$ by $\mathbf{div}_h\, \boldsymbol{\tau}|_K = \mathbf{div}(\boldsymbol{\tau}|_K)$ for all $K \in \mathcal{T}_h$ and we endow $\boldsymbol{\mathcal{V}}(h) := \boldsymbol{\mathcal{V}} + \boldsymbol{\mathcal{V}}_h$ with the following seminorm

$$|\boldsymbol{\tau}|^2_{\boldsymbol{\mathcal{V}}(h)} := \|\mathbf{div}_h\, \boldsymbol{\tau}\|^2_{0,\Omega} + \|h_{\mathcal{F}}^{-1/2}[\![\boldsymbol{\tau}]\!]\|^2_{0,\mathcal{F}_h^*},$$

which is well defined in $\boldsymbol{\mathcal{V}}(h)$ and the norm

$$\|\boldsymbol{\tau}\|^2_{\mathrm{DG}} := |\boldsymbol{\tau}|^2_{\boldsymbol{\mathcal{V}}(h)} + \|\boldsymbol{\tau}\|^2_{0,\Omega}.$$

In our analysis, we will need the following discrete trace inequality (see [10])

$$\|h^{1/2}\{v\}\|_{0,\mathcal{F}} \leq C\|v\|_{0,\Omega} \qquad \forall v \in \mathbb{P}_k(\mathcal{T}_h). \tag{3.9}$$

Now, we introduce the symmetric and non-symmetric DG discretizations to solve the Stokes eigenvalue problem (2.2): Find $\lambda_h \in \mathbb{C}$ and $\mathbf{0} \neq \boldsymbol{\sigma}_h \in \boldsymbol{\mathcal{V}}_h$ such that

$$a_h(\boldsymbol{\sigma}_h, \boldsymbol{\tau}_h) = \lambda_h b(\boldsymbol{\sigma}_h, \boldsymbol{\tau}_h) \quad \forall \boldsymbol{\tau}_h \in \boldsymbol{\mathcal{V}}_h, \tag{3.10}$$

where the bilinear form $a_h : \boldsymbol{\mathcal{V}}_h \times \boldsymbol{\mathcal{V}}_h \to \mathbb{C}$ is defined by

$$\begin{aligned} a_h(\boldsymbol{\sigma}_h, \boldsymbol{\tau}_h) := &\int_\Omega \mathbf{div}_h\, \boldsymbol{\sigma}_h \cdot \mathbf{div}_h\, \boldsymbol{\tau}_h + \int_\Omega \boldsymbol{\sigma}_h^{\mathtt{D}} : \boldsymbol{\tau}_h^{\mathtt{D}} \\ &+ \int_{\mathcal{F}_h^*} \mathtt{a}_S h_{\mathcal{F}}^{-1}\, [\![\boldsymbol{\sigma}_h]\!] \cdot [\![\boldsymbol{\tau}_h]\!] - \int_{\mathcal{F}_h^*} \{\mathbf{div}_h\, \boldsymbol{\sigma}_h\} \cdot [\![\boldsymbol{\tau}_h]\!] - \varepsilon \int_{\mathcal{F}_h^*} \{\mathbf{div}_h\, \boldsymbol{\tau}_h\} \cdot [\![\boldsymbol{\sigma}_h]\!], \end{aligned} \tag{3.11}$$

with $\mathtt{a}_S > 0$ is the so called stabilization parameter and $\varepsilon \in \{-1, 0, 1\}$. As is studied in [1], the Hermitian or non-Hermitian nature of the DG method lies in the choice of ε. If $\varepsilon = 1$ we obtain the classic symmetric interior penalty method (SIP) as the one studied, for example in [16] for the elasticity eigenproblem. If $\varepsilon = -1$ we obtain the non-symmetric interior penalty method (NIP) and if $\varepsilon = 0$ the incomplete interior penalty method (IIP).

Notice that, for $\varepsilon = 1$ all the eigenvalues of the discrete problem (3.10) are real. On the other hand, in the case of non-symmetric methods is expectable to obtain complex eigenvalues with the discrete method.

For the analysis, we introduce the following norm

$$\|\boldsymbol{\sigma}\|^*_{\mathrm{DG}} := \big(\|\boldsymbol{\sigma}\|^2_{\mathrm{DG}} + \|h_{\mathcal{F}_h}^{1/2}\{\mathbf{div}\, \boldsymbol{\sigma}\}\|^2_{0,\mathcal{F}_h^*}\big)^{1/2}.$$

It is easy to check that for all $\boldsymbol{\sigma}, \boldsymbol{\tau} \in \boldsymbol{\mathcal{V}}(h)$, and $\mathbf{div}\, \boldsymbol{\sigma}, \mathbf{div}\, \boldsymbol{\tau} \in \mathrm{H}^t(\Omega)^n$ with $t > 1/2$, the bilinear form $a_h(\cdot, \cdot)$ is bounded. In fact, there exists a constant $C > 0$, independent of h, such that

$$\big|a_h(\boldsymbol{\sigma}, \boldsymbol{\tau})\big| \leq C\|\boldsymbol{\sigma}\|^*_{\mathrm{DG}}\|\boldsymbol{\tau}\|^*_{\mathrm{DG}}. \tag{3.12}$$

Moreover, by means of (3.9) is possible to prove that for all $\boldsymbol{\tau}_h \in \boldsymbol{\mathcal{V}}_h$ there exists a positive constant M_{DG} such that

$$|a_h(\boldsymbol{\sigma}, \boldsymbol{\tau}_h)| \leq M_{\mathrm{DG}} \|\boldsymbol{\sigma}\|^*_{\mathrm{DG}} \|\boldsymbol{\tau}_h\|_{\mathrm{DG}}. \tag{3.13}$$

In order to analyze the discrete eigenvalue problem (3.10), we need to decompose the space $\boldsymbol{\mathcal{V}}_h^c$. With this aim, we consider the following subspace of $\boldsymbol{\mathcal{X}}$ (cf. (2.5)).

$$\boldsymbol{\mathcal{X}}_h := \{\boldsymbol{\tau}_h \in \boldsymbol{\mathcal{V}}_h^c : \ \mathbf{div}\, \boldsymbol{\tau}_h = \mathbf{0}\}.$$

The following result shows the existence of the discrete counterpart of operator $\boldsymbol{P}$ and establishes an approximation estimate.

Lemma 3.1. *There exist a projection $\boldsymbol{P}_h : \boldsymbol{\mathcal{V}}_h^c \to \boldsymbol{\mathcal{V}}_h^c$ with kernel $\boldsymbol{\mathcal{X}}_h$ and a constant $C > 0$, independent of h, such that*

$$\|(\boldsymbol{P} - \boldsymbol{P}_h)\boldsymbol{\tau}_h\|_{\mathbf{div},\Omega} \leq C\, h^s \|\mathbf{div}\, \boldsymbol{\tau}_h\|_{0,\Omega} \quad \forall \boldsymbol{\tau}_h \in \boldsymbol{\mathcal{V}}_h^c,$$

where $s \in (0, 1]$ is such that Proposition 2.1 holds true.

Proof. See [21, Lemma 4.4]. □

The following technical result, proved in [19, Proposition 5.2], will be useful in the forthcoming analysis.

Proposition 3.1. *There exist a projection $\mathcal{I}_h : \boldsymbol{\mathcal{V}}_h \to \boldsymbol{\mathcal{V}}_h^c$ and two constants $\underline{C}, \bar{C} > 0$, independent of h, such that*

$$\underline{C}\, \|\boldsymbol{\tau}\|_{\mathrm{DG}} \leq \left(\|\mathcal{I}_h \boldsymbol{\tau}\|^2_{\mathbf{div},\Omega} + \|h_{\mathcal{F}}^{-1/2} [\![\boldsymbol{\tau}]\!]\|^2_{0,\mathcal{F}_h^*} \right)^{1/2} \leq \bar{C}\ \|\boldsymbol{\tau}\|_{\mathrm{DG}} \quad \forall \boldsymbol{\tau} \in \boldsymbol{\mathcal{V}}_h. \tag{3.14}$$

Moreover, we have that

$$\|\mathbf{div}_h(\boldsymbol{\tau} - \mathcal{I}_h \boldsymbol{\tau})\|^2_{0,\Omega} + \sum_{K \in \mathcal{T}_h} h_K^{-2} \|\boldsymbol{\tau} - \mathcal{I}_h \boldsymbol{\tau}\|^2_{0,K} \leq C\ \|h_{\mathcal{F}}^{-1/2} [\![\boldsymbol{\tau}]\!]\|^2_{0,\mathcal{F}_h^*}, \tag{3.15}$$

with $C > 0$ independent of h.

Now we will prove that $a_h(\cdot, \cdot)$ is elliptic in $\boldsymbol{\mathcal{V}}_h$ for any $\varepsilon \in \{-1, 0, 1\}$.

Lemma 3.2. *For any $\varepsilon \in \{-1, 0, 1\}$, there exists a parameter $\mathtt{a}^* > 0$ such that for all $\mathtt{a}_S \geq \mathtt{a}^*$ there holds*

$$a_h(\boldsymbol{\tau}_h, \boldsymbol{\tau}_h) \geq \alpha_{\mathrm{DG}} \|\boldsymbol{\tau}_h\|^2_{\mathrm{DG}} \qquad \forall \boldsymbol{\tau}_h \in \boldsymbol{\mathcal{V}}_h,$$

where $\alpha_{\mathrm{DG}} > 0$, independent of h.

Proof. First, we have that there exists a positive constant α^c (cf. Lemma 2.1) such that

$$a(\boldsymbol{\tau}_h, \boldsymbol{\tau}_h) \geq \alpha^c \|\boldsymbol{\tau}_h\|^2_{\mathbf{div},\Omega} \qquad \forall \boldsymbol{\tau}_h \in \boldsymbol{\mathcal{V}}_h^c.$$

Hence, there exists an operator $\Theta : \boldsymbol{\mathcal{V}}_h^c \to \boldsymbol{\mathcal{V}}_h^c$ that satisfies $a(\boldsymbol{\tau}_h, \Theta \boldsymbol{\tau}_h) = \alpha^c \|\boldsymbol{\tau}_h\|^2_{\mathbf{div},\Omega}$, with $\|\Theta \boldsymbol{\tau}_h\|_{\mathbf{div},\Omega} \leq \|\boldsymbol{\tau}_h\|_{\mathbf{div},\Omega}$.

Let $\boldsymbol{\tau}_h \in \boldsymbol{\mathcal{V}}_h$ which we decompose as follows $\boldsymbol{\tau}_h := \widetilde{\boldsymbol{\tau}}_h + \boldsymbol{\tau}_h^c$ with $\boldsymbol{\tau}_h^c := \mathcal{I}_h \boldsymbol{\tau}_h \in \boldsymbol{\mathcal{V}}_h^c$. Hence

$$a_h(\boldsymbol{\tau}_h, \Theta \boldsymbol{\tau}_h^c + \widetilde{\boldsymbol{\tau}}_h) = \alpha^c \|\boldsymbol{\tau}_h^c\|^2_{\mathbf{div},\Omega} + a_h(\boldsymbol{\tau}_h^c, \widetilde{\boldsymbol{\tau}}_h) + a_h(\widetilde{\boldsymbol{\tau}}_h, \Theta \boldsymbol{\tau}_h^c) + a_h(\widetilde{\boldsymbol{\tau}}_h, \widetilde{\boldsymbol{\tau}}_h). \tag{3.16}$$

Hence, we need to bound the last three terms on the right hand side of the above equality. For the last term of the right hand side we have

$$\begin{aligned}
a_h(\widetilde{\boldsymbol{\tau}}_h,\widetilde{\boldsymbol{\tau}}_h) &= \|\mathbf{div}_h\,\widetilde{\boldsymbol{\tau}}_h\|^2_{0,\Omega}+\|\widetilde{\boldsymbol{\tau}}_h^{\mathtt{D}}\|^2_{0,\Omega}+\mathtt{a}_S\|h_{\mathcal{F}}^{-1/2}[\![\widetilde{\boldsymbol{\tau}}_h]\!]\|^2_{0,\mathcal{F}_h^*}\\
&\quad-(1+\varepsilon)\,\|h_{\mathcal{F}_h^*}^{1/2}\{\mathbf{div}_h\,\widetilde{\boldsymbol{\tau}}_h\}\|_{0,\mathcal{F}_h^*}\|h_{\mathcal{F}_h^*}^{-1/2}[\![\widetilde{\boldsymbol{\tau}}_h]\!]\|_{0,\mathcal{F}_h^*},\\
&\geq \mathtt{a}_S\|h_{\mathcal{F}}^{-1/2}[\![\widetilde{\boldsymbol{\tau}}_h]\!]\|^2_{0,\mathcal{F}_h^*}+\left(\frac{1+\varepsilon}{2}\right)\left(-\|h_{\mathcal{F}_h^*}^{1/2}\{\mathbf{div}_h\,\widetilde{\boldsymbol{\tau}}_h\}\|^2_{0,\mathcal{F}_h^*}-\|h_{\mathcal{F}_h^*}^{-1/2}[\![\widetilde{\boldsymbol{\tau}}_h]\!]\|^2_{0,\mathcal{F}_h^*}\right),\\
&= \mathtt{a}_S\|h_{\mathcal{F}}^{-1/2}[\![\boldsymbol{\tau}_h]\!]\|^2_{0,\mathcal{F}_h^*}-\widehat{C}\left(\frac{1+\varepsilon}{2}\right)\|h_{\mathcal{F}_h^*}^{-1/2}[\![\boldsymbol{\tau}_h]\!]\|^2_{0,\mathcal{F}_h^*},
\end{aligned}$$

where we have used the decomposition $\widetilde{\boldsymbol{\tau}}_h=\boldsymbol{\tau}_h-\boldsymbol{\tau}_h^c$, (3.9) and (3.15). Moreover, $\widehat{C}$ is a constant which depends on the constants of estimates (3.9) and (3.15). Hence

$$a_h(\widetilde{\boldsymbol{\tau}}_h,\widetilde{\boldsymbol{\tau}}_h)\geq(\mathtt{a}_S-C_1)\|h_{\mathcal{F}_h^*}^{-1/2}[\![\boldsymbol{\tau}_h]\!]\|^2_{0,\mathcal{F}_h^*},\tag{3.17}$$

with $C_1=\widehat{C}\left(\dfrac{1+\varepsilon}{2}\right)\geq 0$ independent of h.

Next, we bound $a_h(\boldsymbol{\tau}_h^c,\widetilde{\boldsymbol{\tau}}_h)$ (cf. (3.16)), considering once again the decomposition $\boldsymbol{\tau}_h:=\widetilde{\boldsymbol{\tau}}_h+\boldsymbol{\tau}_h^c$ and applying (3.15) as follows

$$\begin{aligned}
a_h(\boldsymbol{\tau}_h^c,\widetilde{\boldsymbol{\tau}}_h)&\geq-\|\mathbf{div}\,\boldsymbol{\tau}_h^c\|_{0,\Omega}\|\mathbf{div}_h\,\widetilde{\boldsymbol{\tau}}_h\|_{0,\Omega}-\|(\boldsymbol{\tau}_h^c)^{\mathtt{D}}\|_{0,\Omega}\|\widetilde{\boldsymbol{\tau}}^{\mathtt{D}}\|_{0,\Omega}-\|h_{\mathcal{F}_h^*}^{1/2}\{\mathbf{div}\,\boldsymbol{\tau}_h^c\}\|_{0,\mathcal{F}_h^*}\|h_{\mathcal{F}_h^*}^{-1/2}[\![\widetilde{\boldsymbol{\tau}}_h]\!]\|_{0,\mathcal{F}_h^*},\\
&\geq-C_2\|\mathbf{div}\,\boldsymbol{\tau}_h^c\|_{0,\Omega}\|h_{\mathcal{F}_h^*}^{-1/2}[\![\boldsymbol{\tau}_h]\!]\|_{0,\mathcal{F}_h^*}-C_3\|\boldsymbol{\tau}^c\|_{0,\Omega}\|\widetilde{\boldsymbol{\tau}}_h\|_{0,\Omega}-C_4\|\mathbf{div}\,\boldsymbol{\tau}_h^c\|_{0,\Omega}\|h_{\mathcal{F}_h^*}^{-1/2}[\![\boldsymbol{\tau}_h]\!]\|_{0,\mathcal{F}_h^*},\\
&\geq-C_5\|\boldsymbol{\tau}_h^c\|_{\mathbf{div},\Omega}\|h_{\mathcal{F}_h^*}^{-1/2}[\![\boldsymbol{\tau}_h]\!]\|_{0,\mathcal{F}_h^*}.
\end{aligned}$$

Thus,

$$a_h(\boldsymbol{\tau}_h^c,\widetilde{\boldsymbol{\tau}}_h)\geq-\frac{\alpha^c}{4}\|\boldsymbol{\tau}_h^c\|^2_{\mathbf{div},\Omega}-C_6\|h_{\mathcal{F}_h^*}^{-1/2}[\![\boldsymbol{\tau}]\!]\|^2_{0,\mathcal{F}_h^*}.\tag{3.18}$$

On other other hand, to bound $a_h(\widetilde{\boldsymbol{\tau}}_h,\Theta\boldsymbol{\tau}_h^c)$ (cf. (3.16)), we repeat the previous arguments, to obtain that for any $\varepsilon\in\{-1,0,1\}$, there exist $C_7>0$, depending on the constants of estimates (3.9) and (3.15), such that

$$a_h(\widetilde{\boldsymbol{\tau}}_h,\Theta\boldsymbol{\tau}_h^c)\geq C_7\|\boldsymbol{\tau}_h^c\|_{\mathbf{div},\Omega}\|h_{\mathcal{F}_h^*}^{-1/2}[\![\boldsymbol{\tau}_h]\!]\|_{0,\mathcal{F}_h^*},$$

Hence, we obtain that there exists a positive constant C_8 such that

$$a_h(\widetilde{\boldsymbol{\tau}}_h,\Theta\boldsymbol{\tau}_h^c)\geq-\frac{\alpha^c}{4}\|\boldsymbol{\tau}_h^c\|^2_{\mathbf{div},\Omega}-C_8\|h_{\mathcal{F}_h^*}^{-1/2}[\![\boldsymbol{\tau}_h]\!]\|^2_{0,\mathcal{F}_h^*}.\tag{3.19}$$

Now, adding (3.17), (3.18) and (3.19), defining $\mathtt{a}^*:=\dfrac{\alpha^c}{2}+C_9$ with $C_9=C_1+C_6+C_8$ a constant independent of h, choosing $\mathtt{a}_S$ such that $\mathtt{a}_S>\mathtt{a}^*$ and replacing this in (3.16) we obtain

$$a_h(\boldsymbol{\tau}_h,\Theta\boldsymbol{\tau}_h^c+\widetilde{\boldsymbol{\tau}}_h)\geq\frac{\alpha^c}{2}\left(\|\boldsymbol{\tau}_h^c\|_{\mathbf{div},\Omega}+\|h_{\mathcal{F}_h^*}^{-1/2}[\![\boldsymbol{\tau}_h]\!]\|^2_{0,\mathcal{F}_h^*}\right).$$

Finally, applying (3.14) in the last estimate we conclude the proof. □

Remark 3.1. *Notice that Lemma 3.2 holds true for both Hermitian and non Hermitian methods. Moreover, the stability of the DG method depends on some particular stabilization parameter* $\mathtt{a}^*$*. This fact will be relevant for the numerical experiments in the sense that the appearance of possible spurious modes will depend on how small is this parameter.*

Since the bilinear form $a_h(\cdot,\cdot)$ is coercive for any $\varepsilon \in \{-1,0,1\}$, we are in position to introduce the discrete solution operator associated to (3.10):

$$\begin{aligned} \boldsymbol{T}_h^\varepsilon : \boldsymbol{\mathcal{V}} &\to \boldsymbol{\mathcal{V}}_h, \\ \boldsymbol{f} &\mapsto \boldsymbol{T}_h^\varepsilon \boldsymbol{f} := \widetilde{\boldsymbol{\sigma}}_h^\varepsilon, \end{aligned} \tag{3.20}$$

where $\widetilde{\boldsymbol{\sigma}}_h^\varepsilon \in \boldsymbol{\mathcal{V}}_h$ is the unique solution, as a consequence of Lemma 3.2 and the Lax-Milgram Theorem, of the following discrete source problem:

$$a_h(\widetilde{\boldsymbol{\sigma}}_h^\varepsilon, \boldsymbol{\tau}_h) = b(\boldsymbol{f}, \boldsymbol{\tau}_h) \qquad \forall \boldsymbol{\tau}_h \in \boldsymbol{\mathcal{V}}_h.$$

Clearly $\boldsymbol{T}_h^\varepsilon$ is well defined. Moreover, there exists a constant $C > 0$ independent of h such that

$$\|\boldsymbol{T}_h^\varepsilon \boldsymbol{f}\|_{DG} \leq C \|\boldsymbol{f}\|_{\mathbf{div},\Omega} \quad \forall \boldsymbol{f} \in \boldsymbol{\mathcal{V}}.$$

It is easy to check that $(\lambda_h, \boldsymbol{\sigma}_h) \in \mathbb{C} \times \boldsymbol{\mathcal{V}}_h$ is a solution of problem (3.10) if and only if $(\mu_h, \boldsymbol{\sigma}_h) \in \mathbb{C} \times \boldsymbol{\mathcal{V}}_h$ with $\mu_h = 1/\lambda_h$ is an eigenpair of $\boldsymbol{T}_h^\varepsilon$, i.e.

$$\boldsymbol{T}_h^\varepsilon \boldsymbol{\sigma}_h = \frac{1}{\mu_h} \boldsymbol{\sigma}_h.$$

In what follows, we write $\boldsymbol{T}_h$ instead of $\boldsymbol{T}_h^\varepsilon$, for simplicity. The following result gives an approximation property between the continuous and discrete solution operators.

Lemma 3.3. *Let $\boldsymbol{f} \in \boldsymbol{P}(\boldsymbol{\mathcal{V}})$ and $\widetilde{\boldsymbol{\sigma}} := \boldsymbol{T}\boldsymbol{f}$. Then, for any $\varepsilon \in \{-1,0,1\}$*

$$\|(\boldsymbol{T} - \boldsymbol{T}_h)\boldsymbol{f}\|_{\mathrm{DG}} \leq \frac{M_{\mathrm{DG}}}{\alpha_{\mathrm{DG}}} \inf_{\boldsymbol{\tau}_h \in \boldsymbol{\mathcal{V}}_h} \|\boldsymbol{T}\boldsymbol{f} - \boldsymbol{\tau}_h\|_{\mathrm{DG}}^*. \tag{3.21}$$

where M_{DG} and α_{DG} are the constants of (3.13) *and Lemma 3.2, respectively. Moreover, the following estimate*

$$\|(\boldsymbol{T} - \boldsymbol{T}_h)\boldsymbol{f}\|_{\mathrm{DG}} \leq C\, h^s \, \left(\|\widetilde{\boldsymbol{\sigma}}\|_{s,\Omega} + \|\mathbf{div}\, \widetilde{\boldsymbol{\sigma}}\|_{1+s,\Omega}\right), \tag{3.22}$$

holds true with a constant $C > 0$ independent of h and $s \in (0,1]$ as in Proposition 2.1.

Proof. We start by noticing that the DG method is consistent. In fact, we have

$$a_h\big((\boldsymbol{T} - \boldsymbol{T}_h)\boldsymbol{f}, \boldsymbol{\tau}_h\big) = 0 \quad \forall \boldsymbol{\tau}_h \in \boldsymbol{\mathcal{V}}_h. \tag{3.23}$$

Indeed, since $\mathbf{div}\, \widetilde{\boldsymbol{\sigma}} \in \mathrm{H}^{1+s}(\Omega)^n$, we have

$$a_h(\widetilde{\boldsymbol{\sigma}}, \boldsymbol{\tau}_h) = \int_\Omega \mathbf{div}\, \widetilde{\boldsymbol{\sigma}} \cdot \mathbf{div}_h\, \boldsymbol{\tau}_h + \int_\Omega \widetilde{\boldsymbol{\sigma}}^{\mathtt{d}} : \boldsymbol{\tau}_h^{\mathtt{d}} - \int_{\mathcal{F}_h^*} \{\mathbf{div}\, \widetilde{\boldsymbol{\sigma}}\} \cdot [\![\boldsymbol{\tau}_h]\!]. \tag{3.24}$$

It is straightforward to deduce from (2.4)

$$-\nabla\,(\mathbf{div}\, \widetilde{\boldsymbol{\sigma}}) = \boldsymbol{f}^{\mathtt{d}} - \widetilde{\boldsymbol{\sigma}}^{\mathtt{d}}, \tag{3.25}$$

Moreover

$$\begin{aligned} \int_\Omega \mathbf{div}\, \widetilde{\boldsymbol{\sigma}} \cdot \mathbf{div}_h\, \boldsymbol{\tau}_h &= -\sum_{K \in \mathcal{T}_h} \int_K \nabla(\mathbf{div}\, \widetilde{\boldsymbol{\sigma}}) : \boldsymbol{\tau}_h + \sum_{K \in \mathcal{T}_h} \int_{\partial K} \mathbf{div}\, \widetilde{\boldsymbol{\sigma}} \cdot \boldsymbol{\tau}_h \boldsymbol{n}_K \\ &= -\sum_{K \in \mathcal{T}_h} \int_K \nabla(\mathbf{div}\, \widetilde{\boldsymbol{\sigma}}) : \boldsymbol{\tau}_h + \int_{\mathcal{F}_h^*} \{\mathbf{div}\, \widetilde{\boldsymbol{\sigma}}\} \cdot [\![\boldsymbol{\tau}_h]\!]. \end{aligned}$$

Substituting back the last identity and (3.25) into (3.24) we obtain

$$a_h(\widetilde{\boldsymbol{\sigma}}, \boldsymbol{\tau}_h) = b(\boldsymbol{f}, \boldsymbol{\tau}_h) \quad \forall \boldsymbol{\tau}_h \in \boldsymbol{\mathcal{V}}_h.$$

and (3.23) follows.

The Céa estimate (3.21) follows in the usual way by taking advantage of (3.23), the discrete ellipticity, estimate (3.12) and the triangle inequality.

Moreover, we have from (3.21) that

$$\|(\boldsymbol{T} - \boldsymbol{T}_h)\boldsymbol{f}\|_{\mathrm{DG}} \leq \frac{M_{\mathrm{DG}}}{\alpha_{\mathrm{DG}}} \|\widetilde{\boldsymbol{\sigma}} - \Pi_h \widetilde{\boldsymbol{\sigma}}\|^*_{\mathrm{DG}}.$$

Finally, to estimate the term $\|\widetilde{\boldsymbol{\sigma}} - \Pi_h \widetilde{\boldsymbol{\sigma}}\|^*_{DG}$ it is enough to follow the arguments presented in Theorem 4.1 of [16] and using the regularity result provided by Proposition 2.1.

□

The following two lemmas are technical results that will be used to prove convergence of the proposed DG discretization.

Lemma 3.4. *There exists a constant $C > 0$ independent of h, such that for any $\varepsilon \in \{-1, 0, 1\}$ and $\boldsymbol{\tau} \in \boldsymbol{\mathcal{V}}$*

$$\|(\boldsymbol{T} - \boldsymbol{T}_h)\boldsymbol{P}\boldsymbol{\tau}\|_{\mathrm{DG}} \leq C\, h^s\, \|\mathbf{div}\, \boldsymbol{\tau}\|_{0,\Omega},$$

with $s \in (0, 1]$ as in Proposition 2.1.

Proof. The result is a direct consequence of Lemma 3.3 by noticing that $\boldsymbol{T} \circ \boldsymbol{P} \subset \{\boldsymbol{\tau} \in [\mathrm{H}^s(\Omega)^{n\times n}] : \mathbf{div}\, \boldsymbol{\tau} \in \mathrm{H}^{1+s}(\Omega)^n\}$ for $s \in (0, 1]$ due to Proposition 2.1. □

Lemma 3.5. *There exists a constant $C > 0$ independent of h such that*

$$\|(\boldsymbol{T} - \boldsymbol{T}_h)\boldsymbol{\tau}_h\|_{\mathrm{DG}} \leq C\, h^s\, \|\boldsymbol{\tau}_h\|_{\mathrm{DG}} \quad \forall \boldsymbol{\tau}_h \in \boldsymbol{\mathcal{V}}_h.$$

with $s \in (0, 1]$ as in Proposition 2.1.

Proof. For any $\boldsymbol{\tau}_h \in \boldsymbol{\mathcal{V}}_h$ we consider the splitting $\boldsymbol{\tau}_h = \boldsymbol{\tau}_h^c + \widetilde{\boldsymbol{\tau}}_h$ with $\boldsymbol{\tau}_h^c := \mathcal{I}_h \boldsymbol{\tau}_h \in \boldsymbol{\mathcal{V}}_h^c$. We have that

$$(\boldsymbol{T} - \boldsymbol{T}_h)\boldsymbol{\tau}_h = (\boldsymbol{T} - \boldsymbol{T}_h)\widetilde{\boldsymbol{\tau}}_h + (\boldsymbol{T} - \boldsymbol{T}_h)\boldsymbol{\tau}_h^c = (\boldsymbol{T} - \boldsymbol{T}_h)\widetilde{\boldsymbol{\tau}}_h + (\boldsymbol{T} - \boldsymbol{T}_h)\boldsymbol{P}_h\boldsymbol{\tau}_h^c,$$

where the last identity is due to the fact that $(\boldsymbol{I} - \boldsymbol{P}_h)\boldsymbol{\tau}_h^c \in \boldsymbol{\mathcal{X}}_h$ and $\boldsymbol{T} - \boldsymbol{T}_h$ vanishes identically on this subspace. It follows that

$$(\boldsymbol{T} - \boldsymbol{T}_h)\boldsymbol{\tau}_h = (\boldsymbol{T} - \boldsymbol{T}_h)\widetilde{\boldsymbol{\tau}}_h + (\boldsymbol{T} - \boldsymbol{T}_h)(\boldsymbol{P}_h - \boldsymbol{P})\boldsymbol{\tau}_h^c + (\boldsymbol{T} - \boldsymbol{T}_h)\boldsymbol{P}\boldsymbol{\tau}_h^c,$$

Applying triangle inequality with the boundedness of $\boldsymbol{T}$ and $\boldsymbol{T}_h$ we have

$$\begin{aligned}\|(\boldsymbol{T} - \boldsymbol{T}_h)\boldsymbol{\tau}_h\|_{\mathrm{DG}} \leq & \|(\boldsymbol{T} - \boldsymbol{T}_h)\widetilde{\boldsymbol{\tau}}_h\|_{\mathrm{DG}} + \|(\boldsymbol{T} - \boldsymbol{T}_h)(\boldsymbol{P}_h - \boldsymbol{P})\boldsymbol{\tau}_h^c\|_{\mathrm{DG}} + \|(\boldsymbol{T} - \boldsymbol{T}_h)\boldsymbol{P}\boldsymbol{\tau}_h^c\|_{\mathrm{DG}} \\ \leq & \Big(\|\boldsymbol{T}\|_{\mathcal{L}([\mathrm{L}^2(\Omega)^{n\times n}]^2, \boldsymbol{\mathcal{V}})} + \|\boldsymbol{T}_h\|_{\mathcal{L}([\mathrm{L}^2(\Omega)^{n\times n}]^2, \boldsymbol{\mathcal{V}}_h)}\Big)\Big(\|\widetilde{\boldsymbol{\tau}}_h\|_{0,\Omega} + \|(\boldsymbol{P}_h - \boldsymbol{P})\boldsymbol{\tau}_h^c\|_{\mathbf{div},\Omega}\Big) \\ & + \|(\boldsymbol{T} - \boldsymbol{T}_h)\boldsymbol{P}\boldsymbol{\tau}_h^c\|_{DG}.\end{aligned}$$

Using (3.15), Lemma 3.1 and Lemma 3.4 we have that

$$\|\widetilde{\boldsymbol{\tau}}_h\|_{0,\Omega} \leq Ch\|\boldsymbol{\tau}_h\|_{\mathrm{DG}},$$

$$\|(\boldsymbol{P}_h - \boldsymbol{P})\boldsymbol{\tau}_h^c\|_{\mathbf{div},\Omega} \leq Ch^s\|\mathbf{div}\, \boldsymbol{\tau}_h^c\|_{0,\Omega} \leq Ch^s\|\boldsymbol{\tau}_h\|_{\mathrm{DG}}$$

and

$$\|(\boldsymbol{T} - \boldsymbol{T}_h)\boldsymbol{P}\boldsymbol{\tau}_h^c\|_{DG} \leq Ch^s\|\mathbf{div}\, \boldsymbol{\tau}_h^c\|_{0,\Omega} \leq Ch^s\|\boldsymbol{\tau}_h\|_{\mathrm{DG}},$$

respectively, which gives the result. □

4. Convergence and error estimates

In this section we will adapt the results from [8, 9] to establish spectral correctness of the proposed DG method, as well to obtain error estimates for the eigenvalues and eigenfunctions.

Let $\boldsymbol{L} : \boldsymbol{\mathcal{V}}(h) \to \boldsymbol{\mathcal{V}}(h)$ be the operator defined in $\boldsymbol{\mathcal{V}}_h$. We define the norm of this operator by

$$\|\boldsymbol{L}\|_{\mathcal{L}(\boldsymbol{\mathcal{V}}_h,\boldsymbol{\mathcal{V}}(h))} := \sup_{\mathbf{0}\neq\boldsymbol{\tau}_h\in\boldsymbol{\mathcal{V}}_h} \frac{\|\boldsymbol{L}\boldsymbol{\tau}_h\|_{\mathrm{DG}}}{\|\boldsymbol{\tau}_h\|_{\mathrm{DG}}}.$$

As a direct consequence of Lemma 3.4 and the density of smooth functions in $\boldsymbol{\mathcal{V}}$, we have the following properties, P1 and P2, which are all that we need to establish spectral correctness (see [8]) for all the discrete methods (symmetric or non-symmetric).

- P1. $\|\boldsymbol{T} - \boldsymbol{T}_h\|_{\mathcal{L}(\boldsymbol{\mathcal{V}}_h,\boldsymbol{\mathcal{V}}(h))} \to 0$ as $h \to 0$.
- P2. $\forall \boldsymbol{\tau} \in \boldsymbol{\mathcal{V}}$, there holds

$$\inf_{\boldsymbol{\tau}\in\boldsymbol{\mathcal{V}}_h} \|\boldsymbol{\tau} - \boldsymbol{\tau}_h\|_{\mathrm{DG}} \ \to 0 \quad \text{as} \quad h \to 0.$$

As we mention before, the goal of this section is to obtain convergence and error estimates of the DG scheme (see [1, 6, 16] for others DG spectral analysis). In order to do this, first we will prove that the continuous resolvent is bounded in the DG norm.

From now on, $\mathbb{D}$ denotes the unitary disk defined in the complex by $\mathbb{D} := \{z \in \mathbb{C} : |z| \leq 1\}$ where $z \in \mathrm{sp}(\boldsymbol{T})$.

Lemma 4.1. *There exists a constant $C > 0$ independent of h such that for all $z \in \mathbb{D} \setminus \mathrm{sp}(\boldsymbol{T})$ there holds*

$$\|(z\boldsymbol{I} - \boldsymbol{T})\boldsymbol{\tau}\|_{\mathrm{DG}} \geq C|z|\,\|\boldsymbol{\tau}\|_{\mathrm{DG}} \quad \forall \boldsymbol{\tau} \in \boldsymbol{\mathcal{V}}(h)$$

Proof. For $\boldsymbol{\tau} \in \boldsymbol{\mathcal{V}}(h)$, we introduce

$$\boldsymbol{\sigma}^* := \boldsymbol{T}\boldsymbol{\tau} \in \boldsymbol{\mathcal{V}}$$

and notice that

$$(z\boldsymbol{I} - \boldsymbol{T})\boldsymbol{\sigma}^* = \boldsymbol{T}(z\boldsymbol{I} - \boldsymbol{T})\boldsymbol{\tau}.$$

Since $\boldsymbol{T} : \boldsymbol{\mathcal{V}} \to \boldsymbol{\mathcal{V}}$ is a bounded operator and using the fact that $\|(z\boldsymbol{I} - \boldsymbol{T})\,\boldsymbol{\sigma}\|_{\mathbf{div},\Omega} \geq C\|\boldsymbol{\sigma}\|_{\mathbf{div},\Omega}$ for $z \notin \mathrm{sp}(\boldsymbol{T})$ (see Proposition 2.4 in [20] for instance), we have that

$$C\|\boldsymbol{\sigma}^*\|_{\mathbf{div},\Omega} \leq \|(z\boldsymbol{I} - \boldsymbol{T})\boldsymbol{\sigma}^*\|_{\mathbf{div},\Omega} \leq \|\boldsymbol{T}(z\boldsymbol{I} - \boldsymbol{T})\boldsymbol{\tau}\|_{\mathbf{div},\Omega} \leq \|\boldsymbol{T}\|_{\mathcal{L}([\mathrm{L}^2(\Omega)^{n\times n}]^2,\boldsymbol{\mathcal{V}})}\|(z\boldsymbol{I} - \boldsymbol{T})\boldsymbol{\tau}\|_{\mathrm{DG}}.$$

On the other hand, we have

$$\begin{aligned}
\|\boldsymbol{\tau}\|_{\mathrm{DG}} &\leq |z|^{-1}\|\boldsymbol{\sigma}^*\|_{\mathbf{div},\Omega} + |z|^{-1}\|(z\boldsymbol{I} - \boldsymbol{T})\boldsymbol{\tau}\|_{\mathrm{DG}} \\
&\leq |z|^{-1}\left(1 + C\|\boldsymbol{T}\|_{\mathcal{L}([\mathrm{L}^2(\Omega)^{n\times n}]^2,\boldsymbol{\mathcal{V}})}\right)\|(z\boldsymbol{I} - \boldsymbol{T})\boldsymbol{\tau}\|_{\mathrm{DG}} \\
&\leq |z|^{-1}C\|(z\boldsymbol{I} - \boldsymbol{T})\boldsymbol{\tau}\|_{\mathrm{DG}}.
\end{aligned}$$

Hence, $C|z|\|\boldsymbol{\tau}\|_{\mathrm{DG}} \leq \|(z\boldsymbol{I} - \boldsymbol{T})\boldsymbol{\tau}\|_{\mathrm{DG}}$, which conclude the proof. □

Remark 4.1. *Lemma 4.1 implies that the resolvent of $\boldsymbol{T}$ is bounded. This means that there exists a constant $C > 0$ independent of h such that*

$$\|(z\boldsymbol{I} - \boldsymbol{T})^{-1}\|_{\mathcal{L}(\boldsymbol{\mathcal{V}}(h),\boldsymbol{\mathcal{V}}(h))} \leq C. \tag{4.26}$$

Our next goal is to derive the boundedness of the discrete resolvent for h small enough. The following results give us this property and their proofs are not included since are similar to those in Lemma 5.1 and Lemma 5.2 of [16].

Lemma 4.2. *If $z \in \mathbb{D} \setminus \mathrm{sp}(\boldsymbol{T})$, there exists $h_0 > 0$ such that for all $h \leq h_0$,*

$$\|(z\boldsymbol{I} - \boldsymbol{T}_h)\boldsymbol{\tau}_h\|_{\mathrm{DG}} \geq C\,\|\boldsymbol{\tau}_h\|_{\mathrm{DG}} \quad \forall \boldsymbol{\tau}_h \in \boldsymbol{\mathcal{V}}_h,$$

with $C > 0$ independent of h but depending on $|z|$.

Lemma 4.3. *If $z \in \mathbb{D} \setminus \mathrm{sp}(\boldsymbol{T})$, there exists $h_0 > 0$ such that for all $h \leq h_0$,*

$$\|(z\boldsymbol{I} - \boldsymbol{T}_h)\boldsymbol{\tau}\|_{\mathrm{DG}} \geq C\,\|\boldsymbol{\tau}\|_{\mathrm{DG}} \quad \forall \boldsymbol{\tau} \in \boldsymbol{\mathcal{V}}(h),$$

with $C > 0$ independent of h but depending on $|z|^2$.

The previous lemma states that if we consider a compact subset E of the complex plane such that $E \cap \mathrm{sp}(\boldsymbol{T}) = \emptyset$ for h small enough and for all $z \in E$, operator $z\boldsymbol{I} - \boldsymbol{T}_h$ is invertible. Moreover, there exists a positive constant C independent of h such that $\|(z\boldsymbol{I} - \boldsymbol{T}_h)^{-1}\|_{\mathcal{L}(\boldsymbol{\mathcal{V}}(h).\boldsymbol{\mathcal{V}}(h))} \leq C$ for all $z \in E$. This fact is important since determine that the numerical method is spurious free for h *small enough*. This is summarized in the following result proved in [8].

Theorem 4.1. *Let $E \subset \mathbb{C}$ be a compact subset not intersecting $\mathrm{sp}(\boldsymbol{T})$. Then, there exists $h_0 > 0$ such that, if $h \leq h_0$, then $E \cap \mathrm{sp}(\boldsymbol{T}_h) = \emptyset$.*

In order to prove convergence between eigenspaces, we introduce the following definitions: let $\boldsymbol{x} \in \boldsymbol{\mathcal{V}}(h)$ and $\mathbb{E}$ and $\mathbb{F}$ be closed subspaces of $\boldsymbol{\mathcal{V}}(h)$. We define

$$\delta(\boldsymbol{x}, \mathbb{E}) := \inf_{\boldsymbol{y} \in \mathbb{E}} \|\boldsymbol{x} - \boldsymbol{y}\|_{\mathrm{DG}}, \quad \delta(\mathbb{E}, \mathbb{F}) := \sup_{\boldsymbol{y} \in \mathbb{E}:\, \|\boldsymbol{y}\|_{\mathrm{DG}} = 1} \delta(\boldsymbol{y}, \mathbb{F}).$$

Hence, the gap between two closed subspaces is defined by

$$\widehat{\delta}(\mathbb{E}, \mathbb{F}) := \max\{\delta(\mathbb{E}, \mathbb{F}), \delta(\mathbb{F}, \mathbb{E})\}.$$

Let $\kappa \in (0, 1)$ be an isolated eigenvalue of $\boldsymbol{T}$ and let D an open disk in the complex plane with boundary γ such that κ is the only eigenvalue of $\boldsymbol{T}$ lying in D and $\gamma \cap \mathrm{sp}(\boldsymbol{T}) = \emptyset$. We introduce the spectral projector corresponding to the continuous and discrete solution operators $\boldsymbol{T}$ and $\boldsymbol{T}_h$, respectively

$$\boldsymbol{\mathcal{E}} := \frac{1}{2\pi i} \int_\gamma (z\boldsymbol{I} - \boldsymbol{T})^{-1}\, dz : \boldsymbol{\mathcal{V}}(h) \longrightarrow \boldsymbol{\mathcal{V}}(h),$$

$$\boldsymbol{\mathcal{E}}_h := \frac{1}{2\pi i} \int_\gamma (z\boldsymbol{I} - \boldsymbol{T}_h)^{-1}\, dz : \boldsymbol{\mathcal{V}}(h) \longrightarrow \boldsymbol{\mathcal{V}}(h)$$

where $\boldsymbol{\mathcal{E}}_h$ is well-defined and bounded uniformly in h due (4.26). Moreover, $\boldsymbol{\mathcal{E}}|_{\boldsymbol{\mathcal{V}}}$ is a spectral projection in $\boldsymbol{\mathcal{V}}$ onto the (finite dimensional) eigenspace $\boldsymbol{\mathcal{E}}(\boldsymbol{\mathcal{V}})$ corresponding to the eigenvalue κ of $\boldsymbol{T}$. In fact, we have that (see [16] for further details)

$$\boldsymbol{\mathcal{E}}(\boldsymbol{\mathcal{V}}(h)) = \boldsymbol{\mathcal{E}}(\boldsymbol{\mathcal{V}}).$$

Moreover, $\boldsymbol{\mathcal{E}}_h|_{\boldsymbol{\mathcal{V}}_h}$ is a projector in $\boldsymbol{\mathcal{V}}_h$ onto the eigenspace $\boldsymbol{\mathcal{E}}_h(\boldsymbol{\mathcal{V}}_h)$ corresponding to the eigenvalues of $\boldsymbol{T}_h : \boldsymbol{\mathcal{V}}_h \to \boldsymbol{\mathcal{V}}_h$ contained in γ. We also have that

$$\boldsymbol{\mathcal{E}}_h(\boldsymbol{\mathcal{V}}(h)) = \boldsymbol{\mathcal{E}}_h(\boldsymbol{\mathcal{V}}_h).$$

Now, we will compare $\boldsymbol{\mathcal{E}}_h(\boldsymbol{\mathcal{V}}_h)$ to $\boldsymbol{\mathcal{E}}(\boldsymbol{\mathcal{V}})$ in terms of the gap $\widehat{\delta}$. The proof of the next auxiliary result follows from the definition of $\boldsymbol{\mathcal{E}}$ and $\boldsymbol{\mathcal{E}}_h$.

Lemma 4.4. *There exists $C > 0$ independent of h, such that*

$$\|\boldsymbol{\mathcal{E}} - \boldsymbol{\mathcal{E}}_h\|_{\mathcal{L}(\boldsymbol{\mathcal{V}}_h, \boldsymbol{\mathcal{V}}(h))} \leq C \|\boldsymbol{T} - \boldsymbol{T}_h\|_{\mathcal{L}(\boldsymbol{\mathcal{V}}_h, \boldsymbol{\mathcal{V}}(h))}.$$

The following result will be used to establish the approximation properties of the eigenfunctions of the continuous problem by means of those of the discrete DG discretisations.

Lemma 4.5. *There exists a positive constant C independent of h such that*

$$\widehat{\delta}(\boldsymbol{\mathcal{E}}(\boldsymbol{\mathcal{V}}), \boldsymbol{\mathcal{E}}_h(\boldsymbol{\mathcal{V}}_h)) \leq C \Big(\|\boldsymbol{T} - \boldsymbol{T}_h\|_{\mathcal{L}(\boldsymbol{\mathcal{V}}_h, \boldsymbol{\mathcal{V}}(h))} + \delta(\boldsymbol{\mathcal{E}}(\boldsymbol{\mathcal{V}}), \boldsymbol{\mathcal{V}}_h) \Big).$$

Now, we state the convergence properties of the DG methods.

Theorem 4.2. *Let $\kappa \in (0,1)$ be an eigenvalue of $\boldsymbol{T}$ of algebraic multiplicity m and let D_κ be a closed disk in the complex plane centered at κ with boundary γ such that $D_\kappa \cap \mathrm{sp}(\boldsymbol{T}) = \{\kappa\}$. Let $\kappa_{1,h}, \ldots, \kappa_{m(h),h}$ be the eigenvalues of $\boldsymbol{T}_h$ lying in D_κ and repeated according to their algebraic multiplicity. Then, for any DG method defined by $\varepsilon \in \{-1, 0, 1\}$, we have that $m(h) = m$ for h sufficiently small and*

$$\lim_{h \to 0} \max_{1 \leq i \leq m} |\kappa - \kappa_{i,h}| = 0.$$

Moreover, if $\boldsymbol{\mathcal{E}}(\boldsymbol{\mathcal{V}})$ is the eigenspace corresponding to κ and $\boldsymbol{\mathcal{E}}_h(\boldsymbol{\mathcal{V}}_h)$ is the $\boldsymbol{T}_h$-invariant subspace of $\boldsymbol{\mathcal{V}}_h$ spanned by the eigenspaces corresponding to $\{\kappa_{i,h},\ i = 1, \ldots, m\}$ then

$$\lim_{h \to 0} \widehat{\delta}(\boldsymbol{\mathcal{E}}(\boldsymbol{\mathcal{V}}), \boldsymbol{\mathcal{E}}_h(\boldsymbol{\mathcal{V}}_h)) = 0.$$

Proof. See proof of Theorem 5.2 in [16]. □

Remark 4.2. *The above result for the eigenvalues κ of $\boldsymbol{T}$ and $\kappa_{i,h}$ of $\boldsymbol{T}_h$ yield analogous conclusion for the eigenvalues $\lambda = 1/\kappa$ of problem (2.2) and the eigenvalues $\lambda_{i,h} = 1/\kappa_{i,h}$ of problem (3.10).*

Let us introduce the following distance

$$\delta^*(\boldsymbol{\mathcal{E}}(\boldsymbol{\mathcal{V}}), \boldsymbol{\mathcal{V}}_h) := \sup_{\boldsymbol{\tau} \in \boldsymbol{\mathcal{E}}(\boldsymbol{\mathcal{V}}), \|\boldsymbol{\tau}\|_{\mathrm{DG}} = 1} \inf_{\boldsymbol{\tau}_h \in \boldsymbol{\mathcal{V}}_h} \|\boldsymbol{\tau} - \boldsymbol{\tau}_h\|_{\mathrm{DG}}^*.$$

The following results has been proved in [16, Theorem 6.1] for a fixed eigenvalue $\kappa \in (0,1)$ of $\boldsymbol{T}$.

Theorem 4.3. *For h small enough, there exists a positive constant C, independent of h, such that*

$$\widehat{\delta}\big(\boldsymbol{\mathcal{E}}(\boldsymbol{\mathcal{V}}), \boldsymbol{\mathcal{E}}_h(\boldsymbol{\mathcal{V}}_h)\big) \leq C \delta^*(\boldsymbol{\mathcal{E}}(\boldsymbol{\mathcal{V}}), \boldsymbol{\mathcal{V}}_h).$$

Finally, with the aid of Proposition 2.2, we present the rates of convergence of the proposed DG methods.

Theorem 4.4. *Let $r > 0$ be such that $\boldsymbol{\mathcal{E}}(\boldsymbol{\mathcal{V}}) \subset \{\boldsymbol{\tau} \in \mathrm{H}^r(\Omega)^{n \times n} : \mathbf{div}\, \boldsymbol{\tau} \in \mathrm{H}^{1+r}(\Omega)^n\}$ (cf. Proposition 2.2). Then, there exists $C_1, C_2 > 0$, independent of h, such that, for $\varepsilon \in \{-1, 0\}$ we have*

$$\widehat{\delta}(\boldsymbol{\mathcal{E}}_h(\boldsymbol{\mathcal{V}}_h), \boldsymbol{\mathcal{E}}(\boldsymbol{\mathcal{V}})) \leq C_1 h^{\min\{r,k\}}, \tag{4.27}$$

and

$$\max_{1 \leq i \leq m} |\lambda - \lambda_{i,h}| \leq C_2\, h^{\min\{r,k\}}. \tag{4.28}$$

Moreover, if $\varepsilon = 1$, (4.27) holds true and there exists $C_3 > 0$, independent of h, such that

$$\max_{1 \leq i \leq m} |\lambda - \lambda_{i,h}| \leq C_3\, h^{2\min\{r,k\}} \tag{4.29}$$

Proof. To obtain (4.27) we follow the arguments presented in Theorem 6.2 of [16]. Notice that (4.28) is a direct consequence of (4.27).

To prove the double order of convergence in the case $\varepsilon = 1$, we procede as follows: let $\kappa_{1,h}, \ldots, \kappa_{m,h}$ be the eigenvalues of $\boldsymbol{T}_h : \boldsymbol{\mathcal{V}}_h \to \boldsymbol{\mathcal{V}}_h$ lying in D_κ and repeated according to their algebraic multiplicity.

Let $\boldsymbol{\sigma}_{i,h}$ be the eigenfunction corresponding to $\kappa_{i,h}$ and satisfying $\|\boldsymbol{\sigma}_h\|_{\mathrm{DG}} = 1$. We know from Theorem 4.3 that, if h is sufficiently small,

$$\delta(\boldsymbol{\sigma}_h, \boldsymbol{\mathcal{E}}(\boldsymbol{\mathcal{V}})) \leq C\delta^*(\boldsymbol{\mathcal{E}}(\boldsymbol{\mathcal{V}}), \boldsymbol{\mathcal{V}}_h).$$

Then, there exists an eigenfunction $\boldsymbol{\sigma} \in \boldsymbol{\mathcal{E}}(\mathbb{X})$ satisfying

$$\|\boldsymbol{\sigma}_h - \boldsymbol{\sigma}\|_{\mathrm{DG}} = \delta(\boldsymbol{\sigma}_h, \boldsymbol{\mathcal{E}}(\boldsymbol{\mathcal{V}})) \leq \widehat{\delta}(\boldsymbol{\mathcal{E}}_h(\boldsymbol{\mathcal{V}}_h), \boldsymbol{\mathcal{E}}(\boldsymbol{\mathcal{V}})) \leq C\delta^*(\boldsymbol{\mathcal{E}}(\boldsymbol{\mathcal{V}}), \boldsymbol{\mathcal{V}}_h) \to 0,$$

as $h \to 0$ and hence, we prove a lower and upper bound of $\|\boldsymbol{\sigma}\|_{\mathrm{DG}}$ with a constant independent of h.

On the other hand, proceeding as in the proof of the consistency property in Lemma 3.3 we obtain that

$$a_h(\boldsymbol{\sigma}, \boldsymbol{\tau}_h) = \lambda b(\boldsymbol{\sigma}, \boldsymbol{\tau}_h) \quad \forall \boldsymbol{\tau}_h \in \boldsymbol{\mathcal{V}}_h, \tag{4.30}$$

where from now on, we work with the eigenvalues $\lambda = 1/\kappa$ and $\lambda_{i,h} = 1/\kappa_{i,h}$ (cf. Remark 4.2).

Now, with the aid of (4.30), it is easy to show that the identity

$$a_h(\boldsymbol{\sigma} - \boldsymbol{\sigma}_h, \boldsymbol{\sigma} - \boldsymbol{\sigma}_h) - \lambda b(\boldsymbol{\sigma} - \boldsymbol{\sigma}_h, \boldsymbol{\sigma} - \boldsymbol{\sigma}_h) = (\lambda_{i,h} - \lambda)\, b(\boldsymbol{\sigma}_h, \boldsymbol{\sigma}_h)$$

holds true. On the other hand, due Lemma 3.2 we have that

$$b(\boldsymbol{\sigma}_h, \boldsymbol{\sigma}_h) = \frac{a_h(\boldsymbol{\sigma}_h, \boldsymbol{\sigma}_h)}{|\lambda_{i,h}|} \geq \frac{\alpha_{\mathrm{DG}}\|\boldsymbol{\sigma}_h\|^2_{\mathrm{DG}}}{|\lambda_{i,h}|} \geq \widehat{C} > 0.$$

Since $a_h(\cdot,\cdot)$ and $b(\cdot,\cdot)$ are bounded bilinear forms, we have

$$\widehat{C}|\lambda_{i,h} - \lambda| \leq |a_h(\boldsymbol{\sigma} - \boldsymbol{\sigma}_h, \boldsymbol{\sigma} - \boldsymbol{\sigma}_h)| + |\lambda||b(\boldsymbol{\sigma} - \boldsymbol{\sigma}_h, \boldsymbol{\sigma} - \boldsymbol{\sigma}_h)| \leq C(\|\boldsymbol{\sigma} - \boldsymbol{\sigma}_h\|^*_{\mathrm{DG}})^2.$$

By definition of $\|\cdot\|^*_{\mathrm{DG}}$ we have

$$\|\boldsymbol{\sigma} - \boldsymbol{\sigma}_h\|^*_{\mathrm{DG}} = \|\boldsymbol{\sigma} - \boldsymbol{\sigma}_h\|_{\mathrm{DG}} + \|h_{\mathcal{F}}^{1/2}\{\mathbf{div}(\boldsymbol{\sigma} - \boldsymbol{\sigma}_h)\}\|_{\mathcal{F}_h^*}. \tag{4.31}$$

Clearly we have

$$\|\boldsymbol{\sigma} - \boldsymbol{\sigma}_h\|_{\mathrm{DG}} \leq C\delta^*\left(\boldsymbol{\mathcal{E}}(\boldsymbol{\mathcal{V}}), \boldsymbol{\mathcal{V}}_h\right) \leq Ch^{\min\{r,k\}}\left(\|\boldsymbol{\sigma}\|_{r,\Omega} + \|\mathbf{div}\,\boldsymbol{\sigma}\|_{1+r,\Omega}\right) \leq Ch^{\min\{r,k\}}\|\boldsymbol{\sigma}\|_{\mathbf{div},\Omega},$$

where we have used Proposition 2.2.

To bound the second term in (4.31), we follow the arguments in the proof of Theorem 6.2 of [16], which is enough conclude the proof. □

5. Numerical results

This section is dedicated to report some numerical results for the three different DG discretizations to solve the Stokes eigenvalue problem introduced in (3.10) and obtained with $\varepsilon \in \{-1, 0, 1\}$.

These results have been obtained using a FEniCS code [17]. We will present two different situations: The first consists in apply the method to solve the Stokes eigenvalue problem considering mixed boundary conditions to observe if the method introduce spurious eigenvalues. In particular, we will analyze the influence stabilization parameter $\mathtt{a}_S$. We note that others spectral analysis using DG methods introduces spurious eigenvalues (see for instance [16]). On the other hand, in the second test we apply the method considering homogeneous Dirichlet conditions in order to approximate smooth eigenfunctions and obtain rates of convergence. These two scenarios will be tested for the SIP ($\varepsilon = 1$), NIP ($\varepsilon = 0$) and IIP ($\varepsilon = 0$) methods in order to compare them.

From now and on, the stabilization parameter $\mathtt{a}_S$ in the bilinear form $a_h(\cdot,\cdot)$ in problem (3.10) will be chosen proportionally to the square of the polynomial degree k as $\mathtt{a}_S = \mathtt{a}k^2$ with $\mathtt{a} > 0$. Also, in the tests we will consider uniform and non-uniform meshes. In the former case, we consider the following meshes.

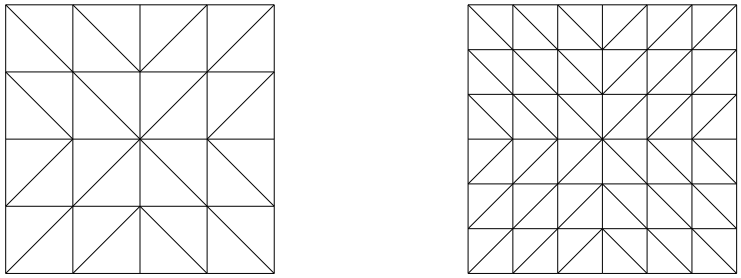

$N = 4$ $N = 6$

Figure 1: Uniform meshes

In Figure 1 the parameter N is the refinement level and is related to the number of elements on each edge. Non-uniform meshes will be considered for certain tests, which are created with the FEniCS command "`generate-mesh`".

5.1. The SIP method

5.1.1. Square domain with mixed boundary conditions.

In the following experiment we will consider the unit square $\Omega := (0,1)^2$ as computational domain. We will impose mixed boundary conditions in the sense that the bottom of the square is Γ_D and the rest of the boundary is Γ_N (cf. (2.1)). We start by determining a reliable stabilization parameter $\mathtt{a}_S$ for the SIP method. This is relevant since according to Lemma 3.2, the DG method is stable when $\mathtt{a}_S > \mathtt{a}^*$. Moreover, we have proved that the spectral correctness is guaranteed if $\mathtt{a}_S$ large enough and the mesh size h is sufficiently small.

In Tables 1, 2, 3 and 4 we report the first ten computed eigenvalues on a fixed uniform mesh with refinement level $N = 8$ and for different values of $\mathtt{a} = 1/2, 1, 2, 4, 8$, obtained with the SIP discrete method and with different polynomial degrees $k = 2, 3, 4, 5$, respectively.

$\mathtt{a} = 1/2$	$\mathtt{a} = 1$	$\mathtt{a} = 2$	$\mathtt{a} = 4$	$\mathtt{a} = 8$
2.4673952	2.4674098	2.4673988	2.4674009	2.4674027
6.2783711	6.2783205	6.2786077	6.2786461	6.2786916
15.2050875	13.8080740	15.2048401	15.2070648	15.2075325
22.2022769	15.2299336	22.2044904	22.2064982	22.2078141
26.9367195	17.3551502	26.9393017	26.9471212	26.9491043
43.1056252	22.2101498	27.2595556	43.1376899	43.1479911
48.2638010	26.9399936	30.8054160	48.3254124	48.3358111
61.5890137	43.1227662	43.1497375	61.6831890	61.7107090
64.1452024	48.3054908	48.3070401	64.2950564	64.3252159
74.9906822	49.7022276	61.6537505	75.1861780	75.2318836

Table 1: Computed eigenvalues for $k = 2$, refinement level of the mesh $N = 8$ and different stabilization values.

$\mathtt{a} = 1/2$	$\mathtt{a} = 1$	$\mathtt{a} = 2$	$\mathtt{a} = 4$	$\mathtt{a} = 8$
2.4674011	2.4674011	2.4674010	2.4674011	2.4674011
6.2791864	6.2791542	6.2791872	6.2791866	6.2791870
15.2086573	6.4680014	15.2086789	15.208673	15.208676
22.2066096	6.5053145	22.2066065	22.206612	22.206614
26.9479205	15.208699	26.9479235	26.947926	26.947935
43.1405126	22.206666	43.1407403	43.140792	43.140827
48.3293767	26.947820	48.3317069	48.331680	48.331792
50.9847437	30.970406	61.6847900	61.685202	61.685275
59.1914865	31.290172	64.2981726	64.298195	64.298384
61.6796639	43.141623	75.1925479	75.192869	75.193319

Table 2: Computed eigenvalues for $k = 3$, refinement level of the mesh $N = 8$ and different stabilization values.

$\mathtt{a} = 1/2$	$\mathtt{a} = 1$	$\mathtt{a} = 2$	$\mathtt{a} = 4$	$\mathtt{a} = 8$
2.4674011	2.4674011	2.4674011	2.4674011	2.4674011
6.2793050	6.2793049	6.2793047	6.2793052	6.2793052
15.2090382	15.2090394	15.2090336	15.2090388	15.2090390
22.2066099	22.2066099	22.2066099	22.2066099	22.2066099
26.9482072	26.9482055	26.9482059	26.9482120	26.9482122
43.1412120	42.2740886	42.7979738	43.1412164	43.1412169
48.3337162	43.1411912	43.1411873	48.3337694	48.3337722
61.6850268	48.3337745	48.3335293	61.6850281	61.6850284
64.2994996	61.6850277	50.2928849	64.2995149	64.2995175
75.1957131	62.7115948	61.6848550	75.1958427	75.1958505

Table 3: Computed eigenvalues for $k = 4$, refinement level of the mesh $N = 8$ and different stabilization values.

$\mathtt{a}=1/2$	$\mathtt{a}=1$	$\mathtt{a}=2$	$\mathtt{a}=4$	$\mathtt{a}=8$
2.4674011	2.4674011	2.4674011	2.4674011	2.4674011
6.2793410	6.2793410	6.2793410	6.2793410	6.2793410
8.7584062	14.7272349	15.2091513	15.2091514	15.2091514
8.9525072	14.7446998	22.2066099	22.2066099	22.2066099
15.2091529	15.2091514	26.9482991	26.9482992	26.9482992
22.2066099	22.2066099	43.1413650	43.1413653	43.1413654
26.9482988	26.9482991	48.3344357	48.3344376	48.3344379
43.1413660	43.1413652	61.6850275	61.6850275	61.6850275
48.3344338	48.3344342	64.3000074	64.3000092	64.3000095
61.6850275	60.9324690	75.1969504	75.1969556	75.1969564

Table 4: Computed eigenvalues for $k = 5$, refinement level of the mesh $N = 8$ and different stabilization values.

In Tables 1, 2, 3 and 4, the eigenvalues inside boxes correspond to spurious eigenvalues. Thus, the present DG method (SIP) introduces spurious eigenvalues if the stabilization parameter is not sufficiently large. We observe from these tables that for all polynomial degrees, when the parameter $\mathtt{a}$ increases, these spurious eigenvalues vanishes from the spectrum. From these results we observe that for $\mathtt{a} = 8$ there is no presence of spurious eigenvalues in all the tables.

5.1.2. Square domain with smooth eigenfunctions.

The aim of this test is to determine the convergence rate of the SIP method. For this numerical experiment we consider the square domain $\Omega := (-1, 1)^2$ as computational domain. We will consider the boundary condition $\boldsymbol{u} = \mathbf{0}$ on the whole boundary.

We report in Table 5 the six lowest eigenvalues computed with the SIP method and with $\mathtt{a} = 10$ (to avoid the presence of possible spurious eigenvalues). The polynomial degrees are given by $k = 1, 2, 3$. We consider non-uniform meshes with $N = 10, 20, 30, 40$. The table includes orders of convergence as well as accurate values extrapolated by means of a least-squares fitting. In the two last columns of the table, we show the values obtained by extrapolating those computed with different finite element methods, applied to solve the same problem, presented in [21] and [18], respectively.

k	$N=10$	$N=20$	$N=30$	$N=40$	Order	λ_{extr}	[21]	[18]
1	13.23530	13.12312	13.10301	13.09557	2.03	13.08683	13.0860	13.086
	23.46703	23.14735	23.08195	23.06083	1.88	23.02751	23.0308	23.031
	23.48255	23.14789	23.08326	23.06087	1.94	23.02986	23.0308	23.031
	32.91691	32.28099	32.15261	32.10993	1.89	32.04518	32.0443	32.053
	39.73787	38.85144	38.67522	38.61419	1.90	38.52632	38.5252	38.532
	43.21970	42.14111	41.92730	41.85513	1.91	41.74927	41.7588	41.759
2	13.08798	13.08629	13.08619	13.08618	3.94	13.08617	13.0860	13.086
	23.04090	23.03171	23.03122	23.03113	3.99	23.03109	23.0308	23.031
	23.04164	23.03172	23.03123	23.03113	4.08	23.03110	23.0308	23.031
	32.07787	32.05408	32.05274	32.05250	3.92	32.05239	32.0443	32.053
	38.57979	38.53426	38.53194	38.53154	4.07	38.53138	38.5252	38.532
	41.80864	41.76061	41.75795	41.75750	3.95	41.75728	41.7588	41.759
3	13.08618	13.08617	13.08617	13.08617	6.19	13.08617	13.0860	13.086
	23.03117	23.03109	23.03109	23.03109	5.92	23.03109	23.0308	23.031
	23.03118	23.03109	23.03109	23.03109	6.10	23.03109	23.0308	23.031
	32.05276	32.05240	32.05239	32.05239	6.10	32.05239	32.0443	32.053
	38.53189	38.53137	38.53136	38.53136	5.92	38.53136	38.5252	38.532
	41.75803	41.75730	41.75729	41.75729	6.00	41.75729	41.7588	41.759

Table 5: Lowest computed eigenvalues for polynomial degrees $k = 1, 2, 3$, $\mathtt{a} = 10$.

In this case, since Ω is convex, the problem have smooth eigenfunctions, as a consequence, when using polinomial degree k, the order of convergence is $2k$ as the theory predicts (cf. Theorem 4.4). Moreover, the results obtained by the three methods agree perfectly well.

5.2. The NIP method

Let us recall that the NIP method is obtained by taking $\varepsilon = -1$ in (3.11). The first tests consists in the observation of spurious eigenvalues with the NIP method. As in the SIP method, we know that the appearance of spurious eigenvalues depend on the choice of the stabilization parameter, so we are interested in determine a reliable value of $\mathtt{a}_S$ and compare it with the observed for the SIP method.

In this numerical test, we take the same configuration of the problem as in Section 5.1.1. We also consider different polynomial degress and once more, we fix $N = 8$ as refinement level for the mesh.

$\mathtt{a} = 1/16$	$\mathtt{a} = 1/8$	$\mathtt{a} = 1/4$	$\mathtt{a} = 1/2$	$\mathtt{a} = 1$
2.4721900	2.4719820	2.4716086	2.4710183	2.4702292
6.2867722	6.2876798	6.2874953	6.2864875	6.2848802
15.3436563	15.3430793	15.3344816	15.3178801	15.2945247
22.5758800	22.5672129	22.5403719	22.4944190	22.4320860
27.2535812	27.2705417	27.2565378	27.2183176	27.1617122
44.4811198	44.4559551	44.3741072	44.2123471	43.9860753
47.8366427	49.1414414	49.1512947	49.0631795	48.9128539
47.8658246	64.2105023	64.1241730	63.8165901	63.3669044
47.8658246	66.4074400	66.3880515	66.1610536	65.7894196
48.2260686	78.1827930	78.1523273	77.8113776	77.2682228

Table 6: Computed eigenvalues for $k = 2$, refinement level of the mesh $N = 8$ and different stabilization values.

$\mathtt{a} = 1/16$	$\mathtt{a} = 1/8$	$\mathtt{a} = 1/4$	$\mathtt{a} = 1/2$	$\mathtt{a} = 1$
2.4674071	2.4674061	2.4674050	2.4674039	2.4674030
6.2791238	6.2791444	6.2791633	6.2791814	6.2791947
15.2097172	15.2096509	15.2095048	15.2093382	15.2091780
22.2109165	22.2102393	22.2094497	22.2086809	22.2080315
26.9498165	26.9498169	26.9496152	26.9493860	26.9491478
43.1701050	43.1662597	43.1612684	43.1561487	43.1516245
48.3415270	48.3435730	48.3429551	48.3415116	48.3397671
61.7736247	61.7598178	61.7440082	61.7284035	61.7149867
64.3766118	64.3702919	64.3580404	64.3442239	64.3314399
75.2957059	75.2925537	75.2776318	75.2593133	75.2416689

Table 7: Computed eigenvalues for $k = 3$, refinement level of the mesh $N = 8$ and different stabilization values.

$\mathtt{a} = 1/16$	$\mathtt{a} = 1/8$	$\mathtt{a} = 1/4$	$\mathtt{a} = 1/2$	$\mathtt{a} = 1$
2.4674007	2.4674008	2.4674008	2.4674008	2.4674009
6.2793114	6.2793111	6.2793103	6.2793092	6.2793081
15.2090047	15.2090065	15.2090084	15.2090117	15.2090170
22.2063854	22.2063998	22.2064222	22.2064539	22.2064926
26.9480089	26.9480258	26.9480473	26.9480762	26.9481107
43.1396640	43.1397720	43.1399213	43.1401316	43.1403915
48.3327684	48.3328818	48.3330010	48.3331479	48.3333152
61.6804055	61.6807669	61.6812586	61.6819186	61.6826970
64.2956445	64.2959311	64.2962817	64.2967717	64.2973955
75.1890992	75.1897554	75.1904693	75.1913947	75.1925052

Table 8: Computed eigenvalues for $k = 4$, refinement level of the mesh $N = 8$ and different stabilization values.

We observe in Tables 6, 7 and 8 that, contrary to what happened with the SIP method for the same problem, the NIP method needs smaller stabilization parameter to avoid spurious eigenvalues. Moreover, clearly spurious eigenvalues vanish when we increase the polynomial degree, leaving the physical spectrum clean. This phenomenon does not occur with the symmetric method, and it is a clear advantage to calculate the physical eigenvalues.

Now, our aim is to analyze the order convergence of the NIP method. With this goal, we consider the same computational domain and boundary conditions as in Section 5.1.2.

We report in Table 9 the six lowest eigenvalues computed with the NIP method and with $\mathtt{a} = 2$. The polynomial degrees are given by $k = 1, 2, 3, 4$. We consider uniform meshes with $N = 10, 20, 30, 40$. The table includes orders of convergence as well as accurate values extrapolated by means of a least-squares fitting. In the two last columns of the table, we show the values obtained by extrapolating those computed with different finite element methods presented in [21] and [18], respectively.

k	$N=10$	$N=20$	$N=30$	$N=40$	Order	λ_{extr}	[21]	[18]
1	12.28911	12.88060	12.99430	13.03440	1.94	13.08900	13.0860	13.086
	20.31663	22.30382	22.70387	22.84625	1.87	23.05260	23.0308	23.031
	20.94590	22.49347	22.79091	22.89575	1.94	23.03865	23.0308	23.031
	27.57492	30.83654	31.50459	31.74283	1.85	32.09233	32.0443	32.053
	31.97605	36.76939	37.73881	38.08373	1.87	38.58001	38.5252	38.532
	34.19537	39.69930	40.82883	41.23233	1.84	41.83386	41.7588	41.759
2	13.22024	13.12045	13.10147	13.09479	1.96	13.08590	13.0860	13.086
	23.38718	23.12303	23.07220	23.05427	1.94	23.02991	23.0308	23.031
	23.48972	23.15049	23.08456	23.06124	1.93	23.02951	23.0308	23.031
	32.81717	32.25537	32.14363	32.10392	1.89	32.04759	32.0443	32.053
	39.64207	38.82517	38.66331	38.60583	1.90	38.52547	38.5252	38.532
	43.06625	42.10278	41.91235	41.84481	1.90	41.74981	41.7588	41.759
3	13.08747	13.08625	13.08619	13.08618	3.98	13.08617	13.0860	13.086
	23.03624	23.03143	23.03116	23.03112	3.96	23.03110	23.0308	23.031
	23.03946	23.03163	23.03120	23.03113	3.97	23.03110	23.0308	23.031
	32.07150	32.05363	32.05264	32.05247	3.95	32.05239	32.0443	32.053
	38.56114	38.53330	38.53175	38.53149	3.94	38.53136	38.5252	38.532
	41.79517	41.75974	41.75778	41.75745	3.95	41.75729	41.7588	41.759
4	13.08606	13.086	13.08617	13.08617	3.89	13.08617	13.0860	13.086
	23.03042	23.031	23.03109	23.03110	3.80	23.03110	23.0308	23.031
	23.03067	23.031	23.03109	23.03110	3.83	23.03110	23.0308	23.031
	32.05094	32.052	32.05237	32.05239	3.69	32.05240	32.0443	32.053
	38.52909	38.531	38.53133	38.53135	3.71	38.53137	38.5252	38.532
	41.75444	41.757	41.75725	41.75728	3.71	41.75730	41.7588	41.759

Table 9: Lowest computed eigenvalues for polynomial degrees $k = 1, 2, 3, 4$, $\mathtt{a} = 2$.

We observe in this case that the order of convergence depends on the polinomial degree. However, we observe in the column λ_{extr} that the computed extrapolated values converge to those in the reference columns. More precisely, with respect to the convergence rates, we note that when the polynomial degree is even, the order convergence is $\mathcal{O}(h^k)$ as the theory predicts (cf. (4.28)). We observe that in this case the eigenfunctions are smooth. On the other hand, for odd polynomial degrees we see a superconvergence of the scheme (the order is $\mathcal{O}(h^{k+1})$). This fact has been also seen in [5] where a DG method has been analyzed for the Maxwell's eigenvalue problem.

5.3. The IIP method

In this section, we report numerical results using the IIP method to solve the eigenvalue problem. We recall that we obtain the IIP method considering $\varepsilon = 0$ in (3.11). We have repeated the same experiment presented in Section 5.1.1. We have observed that the spurious eigenvalues behave in a similar way as in the NIP case. For that reason, we do not include tables about this subject.

Now, our aim is to analyze the orders convergence of the IIP method to see if the behavior is similar as in NIP method. We take the same configuration of the domain as in Section 5.1.2.

We report in Table 10 the six lowest eigenvalues computed with the IIP method and with $\mathtt{a} = 2$. The polynomial degrees are given by $k = 1, 2, 3, 4$. Once again, we used uniform meshes with $N = 10, 20, 30, 40$. The table includes orders of convergence as well as accurate values extrapolated by means of a least-squares fitting. In the two last columns of the table, we show the values obtained by extrapolating those computed with different finite element methods presented in [21] and [18], respectively.

k	$N=10$	$N=20$	$N=30$	$N=40$	Order	λ_{extr}	[21]	[18]
1	12.15236	12.84090	12.97615	13.02409	1.91	13.09081	13.0860	13.086
	19.95157	22.17805	22.64447	22.81211	1.81	23.06783	23.0308	23.031
	20.58540	22.38289	22.73984	22.86663	1.89	23.04710	23.0308	23.031
	26.97658	30.61619	31.39938	31.68215	1.77	32.12968	32.0443	32.053
	31.16720	36.45615	37.58787	37.99639	1.78	38.63512	38.5252	38.532
	33.26501	39.33555	40.65254	41.13008	1.76	41.88800	41.7588	41.759
2	13.19299	13.11334	13.09828	13.09299	1.97	13.08602	13.0860	13.086
	23.31856	23.10478	23.06399	23.04963	1.95	23.03021	23.0308	23.031
	23.39557	23.12509	23.07311	23.05477	1.94	23.02980	23.0308	23.031
	32.66925	32.21382	32.12475	32.09321	1.92	32.04989	32.0443	32.053
	39.42492	38.76485	38.63596	38.59036	1.92	38.52748	38.5252	38.532
	42.80949	42.03174	41.88019	41.82660	1.92	41.75238	41.7588	41.759
3	13.08720	13.08624	13.08619	13.08618	3.98	13.08617	13.0860	13.086
	23.03516	23.03136	23.03115	23.03111	3.96	23.03111	23.0308	23.031
	23.03766	23.03152	23.03118	23.03113	3.96	23.03111	23.0308	23.031
	32.06743	32.05337	32.05259	32.05246	3.94	32.05239	32.0443	32.053
	38.55471	38.53289	38.53167	38.53146	3.93	38.53136	38.5252	38.532
	41.78697	41.75922	41.75768	41.75742	3.94	41.75729	41.7588	41.759
4	13.08609	13.08617	13.08617	13.08617	3.90	13.08617	13.0860	13.086
	23.03059	23.03106	23.03109	23.03110	3.82	23.03110	23.0308	23.031
	23.03078	23.03108	23.03109	23.03110	3.85	23.03110	23.0308	23.031
	32.05130	32.05231	32.05238	32.05239	3.73	32.05240	32.0443	32.053
	38.52967	38.53124	38.53134	38.53136	3.73	38.53137	38.5252	38.532
	41.75516	41.75713	41.75726	41.75728	3.73	41.75730	41.7588	41.759

Table 10: Lowest computed eigenvalues for polynomial degrees $k=1,2,3,4$, $\mathtt{a}=2$.

We observe from Table 10 the same behavior as in NIP method (cf. Table 9). More precisely, it can be seen that for even polynomial degrees, the order of convergence is $\mathcal{O}(h^k)$ and for odd polynomial degrees we observe a superconvergence $\mathcal{O}(h^{k+1})$. Once again, the results obtained by this method agree perfectly well with the ones reported in the references.

Remark 5.1. *For the NIP and IIP (non-symmetric) methods we have used uniform meshes to solve the discrete eigenvalue problem and in this case we have obtained only real eigenvalues. We have also tested the methods with non-uniform meshes and we have observed the presence of complex eigenvalues with an imaginary part close to zero. This has been also observed in other DG spectral analysis (see for instance [5]).*

6. Conclusions

We have presented DG discretizations (symmetric and non-symmetric) to solve the Stokes eigenvalue problem where the pseudostress tensor is the unknown. We have established spectral correctness for large enough stabilization parameter and sufficiently small meshsize h. We have seen that the methods introduce spurious eigenvalues for small values of the stabilization parameter. Moreover, we have show that for large enough stabilization parameter, the spurious eigenvalues vanishes for all the methods. In fact, for the SIP method (symmetric) the spurious eigenvalues needs a larger stabilization parameter to avoid the spurious modes compared with the NIP and IIP methods (non-symmetric). We have obtained error estimates for eigenfunctions and eigenvalues for each method. In particular, we have prove a double order of convergence for the SIP method. We have seen a superconvergence for the NIP and IIP methods in the case of odd polynomial degrees.

Aknowledgments

The authors are deeply grateful to Prof. Salim Meddahi (Universidad de Oviedo, Spain) and Prof. Rodolfo Rodríguez (Universidad de Concepción, Chile) for the fruitful discussions.

The first author was partially supported by Proyecto Plurianual 2016-2010 of Universidad del Bío-Bío (Chile) and CONICYT-Chile through FONDECYT Postdoctorado fellowship 3190204 (Chile). The second author was partially supported by CONICYT-Chile through FONDECYT project 1180913 (Chile) and by CONICYT-Chile through the project AFB170001 of the PIA Program: Concurso Apoyo a Centros Científicos y Tecnológicos de Excelencia con Financiamiento Basal.

References

[1] P.F. Antonietti, A. Buffa and I. Perugia, *Discontinuous Galerkin approximation of the Laplace eigenproblem*, Comput. Methods Appl. Mech. Engrg., 195 (2006), pp. 3483–3503.

[2] D. Boffi, Finite element approximation of eigenvalue problems. Acta Numerica, 19 (2010), pp. 1–120.

[3] D. Boffi, F. Brezzi and M. Fortin, Mixed Finite Element Methods and Applications. Springer Series in Computational Mathematics, vol. 44. Springer, Heidelberg, 2013.

[4] F. Brezzi, J.Jr. Douglas and L.D. Marini, *Two families of mixed finite elements for second order elliptic problems*, Numer. Math., 47 (1985), pp. 217–235.

[5] A. Buffa, P. Houston and I. Perugia, *Discontinuous Galerkin computation of the Maxwell eigenvalues on simplicial meshes,* J. Comput. Appl. Math., 2014 (2007), pp. 317–333.

[6] A. Buffa and I. Perugia, *Discontinuous Galerkin approximation of the Maxwell eigenproblem*, SIAM J. Numer. Anal., 44 (2006), pp. 2198–2226.

[7] Z. Cai, Ch. Tong, P.S. Vassilevski and Ch. Wang, *Mixed finite element methods for incompressible flow: stationary Stokes equations*. Numer. Methods Partial Differential Equations, 26 (2010), pp. 957-978.

[8] J. Descloux, N. Nassif and J. Rappaz, *On spectral approximation. Part 1: The problem of convergence*, RAIRO Anal. Numér., 12 (1978), pp. 97–112.

[9] J. Descloux, N. Nassif and J. Rappaz, *On spectral approximation. Part 2: Error estimates for the Galerkin method*, RAIRO Anal. Numér., 12 (1978), pp. 113–119.

[10] D.N. Di Pietro and A. Ern, Mathematical Aspects of Discontinuous Galerkin Methods. Springer-Verlag Berlin Heidelberg 2012.

[11] G.N. Gatica, A. Márquez and M.A. Sánchez, *Analysis of a velocity-pressure-pseudostress formulation for the stationary Stokes equations*, Comput. Methods Appl. Mech. Engrg., 199 (2010), pp. 1064–1079.

[12] G.N. Gatica, A. Márquez, and M.A. Sánchez, *Pseudostress-based mixed finite element methods for the Stokes problem in $\mathbb{R}^n$ with Dirichlet boundary conditions. I: A priori error analysis*, Commun. Comput. Phys., 12 (2012), pp. 109–134.

[13] J. Gedicke and A. Khan, *Arnold-Winther mixed finite elements for Stokes eigenvalue problems*, SIAM J. Sci. Comput., 40 (2018), pp. A3449–A3469.

[14] J. Gedicke and A. Khan, *Divergence-conforming discontinuous Galerkin finite elements for Stokes eigenvalue problems*, arXiv:1805.08981v1, (2018), `https://arxiv.org/abs/1805.08981`

[15] P. Huang, *Lower and upper bounds of Stokes eigenvalue problem based on stabilized finite element methods*, Calcolo, 52 (2015), pp. 109–121.

[16] F. Lepe, S. Meddahi, D. Mora and R. Rodríguez, *Mixed discontinuous Galerkin approximation of the elasticity eigenproblem*, Numer. Math., https://doi.org/10.1007/s00211-019-01035-9 (2019), (to appear).

[17] A. Logg, K.-A. Mardal, G. N. Wells et al. Automated Solution of Differential Equations by the Finite Element Method. Springer 2012.

[18] C. Lovadina, M. Lyly and R. Stenberg *A posteriori estimates for the Stokes eigenvalue problem*, Numer. Methods Partial Differential Equations, 25(1) (2009), pp. 244–257.

[19] A. Márquez, S. Meddahi and T. Tran, *Analyses of mixed continuous and discontinuous Galerkin methods for the time harmonic elasticity problem with reduced symmetry*, SIAM J. Sci. Comput., 37 (2015), pp. 1909–1933.

[20] S. Meddahi, D. Mora and R. Rodríguez, *Finite element spectral analysis for the mixed formulation of the elasticity equations*, SIAM J. Numer. Anal., 51 (2013), pp. 1041–1063.

[21] S. Meddahi, D. Mora and R. Rodríguez, *A finite element analysis of a pseudostress formulation for the Stokes eigenvalue problem*, IMA J. Numer. Anal., 35 (2015), pp. 749–766.

[22] B. Mercier, J. Osborn, J. Rappaz and P.A. Raviart, *Eigenvalue approximation by mixed and hybrid methods*, Math. Comp., 36 (1981), pp. 427–453.

[23] O. Türk, D. Boffi and R. Codina, *A stabilized finite element method for the two-field and three field Stokes eigenvalue problems*, Comput. Methods Appl. Mech. Engrg., 310 (2016), pp. 886–905